

8. REFERENCES

1. Tzanakis ES, Hess DJ, Sielaff TD, Hu WS. Extracorporeal tissue engineered liver assist devices. *Annu Rev Biomed Eng.* 2000;2:607-32.
2. Nahmias Y, Berthiaume F, Yarmush ML. Integration of technologies for hepatic tissue engineering *Adv Biochem Engin/Biotechnol* 2006;103:309-29.
3. Karp SJ. Clinical implications of advances in the basic science of liver repair and regeneration. *Am J Transplant* 2009;9:1973-80.
4. Michalopoulos GK. Liver regeneration: Alternative epithelial pathways. *Int J Biochem Cell Biol* 2009 doi:10.1016/j.biocel.2009.09.014.
5. Sosef MN, Abrahamse LSL, van de Kerkhove MP, Hartman R, Chamuleau RAFM, van Gulik TM. Assessment of the AMC-Bio-artificial Liver in the Anhepatic Pig. *Transplantation.* 2002;73(2):204-9.
6. Bernal W, Wendon J. Acute liver failure: clinical features and management. *Eur J Gastroenterol Hepatol.* 1999;11:977-82.
7. Bismuth H, Figuero J, Samuel D. What we should expect from a bio-artificial liver in fulminant hepatic failure? *Artif Organs.* 1998;22(1):26-31.
8. Bingaman WE, Frank JI. Malignant cerebral edema and intracranial hypertension. *Clin Neurol* 1995;13:479-509.
9. Matsushita M, Nosé Y. Artificial Liver. *Artif Organs.* 1986;10(5):378-84.
10. Moolman FS, Rolfes H, van der Merwe SW, Focke WW. Optimization of Perfluorocarbon emulsion properties for enhancing oxygen mass transfer in a bio-artificial liver support system. *Biochem Eng J.* 2004;19:237-50.
11. Doran PM editor. Process Modeling. In: Bioprocess engineering principles, London Academic Press, 1995, Chapter 13. p.348-52.
12. Cloete A. A new approach to the adult respiratory distress syndrome. (dissertation) University of Cape Town; 1986.
13. Trey C, Davidson CS. The management of fulminant hepatic failure. In: Popper H, Schaffner F (eds) Progress in liver failure. NY, Grune and Stratton 1970;282-298.
14. Bernau J, Rueff B, Benhamou JP. Fulminant and sub-fulminant hepatic failure: definition and causes. *Semin Liver Dis.* 1986;6:97-106.
15. O'Grady JG. Acute Liver Failure. *Postgrad Med J.* 2005;81:148-54 doi:10.1136/pgmj.2004.026005.
16. Riordan SM, Williams R. Perspectives on liver failure: Past and future. *Semin iv Dis* 2008;28:137-41.
17. Lee WM, Squires RH, Nyberg SL, Doo E, Hoofnagle JH. Acute liver failure: Summary of a workshop. *Hepatology* 2008;47(4):1401-15.
18. Sussman, NL, Kelly, J.H. Extracorporeal Liver Support: Cell-Based Therapy for the Failing Liver. *Am J Kidney Dis.* 1997; 30(5):Suppl.4:S66-71.
19. van der Merwe S.W. Gastroenterologist: Unitas hospital, Pretoria, South Africa 2005. Personal communication.
20. van de Kerkhove MP, Hoekstra R, Chamuleau RAFM, van Gulik TM. Clinical application of bio-artificial liver support systems. *Annals Surg.* 2004;240(2):216-30.
21. United network for organ sharing. Liver transplantation data, available at www.unos.org. accessed 2003-6.



22. Mandala L, Pietrosi G, Gruttadauria S, Vizzini G, Spampinato M, Spada M, Gridelli B. Successful liver transplant in an HCV-infected haemophiliac patient with fulminant hepatic failure. *Haemophilia* 2007;13(6):767-9.
23. Taliani G, Tozzi A, Fanci R, Biliotti E, Bsi A. Fatal acute hepatitis C virus infection in patients with haematological malignancies. *J Chemother* 2007;18(6):662-4.
24. Gill RQ, Sterling RK. Acute Liver Failure. *J Clin Gastroenterol.* 2001;33(3):191-8.
25. Rahman T, Hodgson H. Clinical management of acute hepatic failure. *Intensive care Med.* 2001;27:467-76.
26. Bernal W, Auzinger G, Sizer E, Wendon J. Review: Intensive care management of acute liver failure. *Semin Liver Dis.* 2008;28(2):188-200.
27. Haussinger D, Schliess F. Pathogenetic mechanisms of hepatic encephalopathy. *Gut* 2008;57:1156-65.
28. Lichter-Konecki U. Profiling of astrocyte properties in the hyperammonemic brain: Shedding new light on the pathophysiology of the brain damage in hyperammonemia. *J Inherit Metab Dis* 2008;31:492-502.
29. Schliess F, Gorg B, Haussinger D. RNA oxidation and zinc in hepatic encephalopathy *Metab Brain Dis* 2009;24:119-34.
30. Stadlbauer V, Wright GAK, Jalan R. Role of artificial liver support in hepatic encephalopathy. *Metab Brain Dis* 2009;24:15-26.
31. Vaquero J, Butterworth RF. Mechanisms of brain edema in acute liver failure and impact of novel therapeutic interventions. *Neurol Res* 2007;29:683-90.
32. Bernal W, Auzinger G, Sizer E, Wendon J. Variation in blood ammonia concentration with site of measurement and evidence of brain and muscle uptake in patients with acute liver failure. Letter to editor. *Liver Int* 2008; 415-7.
33. Clay AS, Hainline BE. Hyperammonemia in the ICU. *Chest* 2007;132:1368-78.
34. Bjerring PN, Hauerberg J, Frederiksen HJ, Jorgensen L, Hansen A, Tofteng F, Larsen FS. Cerebral glutamine concentration and lactate-to-pyruvate ratio in patients with acute liver failure. *Neurocrit Care* 2008;9:3-7.
35. Wright G, Jalan R. Ammonia and inflammation in the pathogenesis of hepatic encephalopathy: Pandora's box?. *Hepatology* 2007;46(2):291-4.
36. Albrecht J, Noreberg MD. Glutamine: A Trojan horse in ammonia toxicity. *Hepatology* 2006;44(4):788-94.
37. Llansola M, Rodrigo R, Monfort P, Montoliu C, Kosenko E, Cauli O, Piedrafita B, Mlili NE, Felipe V. NMDA receptors in hyperammonemia and hepatic encephalopathy. *Metab Brain Dis* 2007;22:321-35.
38. Rodrigo R, Erceg S, Rodriguez-Diaz J, Saez-Valeron J, Piedrafite B, Suarez I, Felipe V. Glutamate induced activation of nitric oxide synthase is impaired in cerebral cortex in vivo in rats with chronic liver failure. *J Neurochem* 2007;102:51-64.
39. Garcia-Ayllon MS, Cauli O, Silveyra MX, Rodrigo R, Candela A, Compan A, Jover R, Perez-Mateo M, Martinez S, Felipe V, Saez-Valero J. Brain cholinergic impairment in liver failure. *Brain* 2008; sept 4:1-11.
40. Rose C, Felipe V. Limited capacity for ammonia removal by brain in chronic liver failure: potential role of nitric oxide. *Metab Brain Dis* 2005;20(4):275-83.
41. Fischer JE, Baldessarini RJ. Pathogenesis and therapy of hepatic coma. In: Progress in Liver disease, Harvard Medical School, 1976 Chapter 23; p.363-397.
42. Vaquero J, Polson J, Chung C, Helenowski I, Schiodt FV, Reisch J and the US ALF study group. Infection and progression of hepatic encephalopathy in acute liver failure. *Gastroenterol.* 2003;125:755-64.

43. O'Grady JG. Paracetamol hepatotoxicity. *J R Soc Med.* 1997;90:368-70.
44. Donovan JP, Shaw BW, Langnas AN, Sorrell MF. Brain water and ALF: the emerging role of intracranial pressure monitoring. *Hepatology.* 1992;16:267-8.
45. Moore K. Renal failure in acute liver failure. *Eur J Gastroenterol Hepatol.* 1999;11(9):967-75.
46. Gines P, Guevara M, Arroyo V, Rodes J. Hepatorenal syndrome. *Lancet.* 2003;362:1819-27.
47. Wiest R, Groszman RJ. Nitric oxide and portal hypertension: its role in the regulation of intrahepatic and splanchnic vascular resistance. *Semin Liver Dis.* 1999;19:411-26.
48. Barada K. Hepatorenal syndrome: pathogenesis and novel pharmacological targets. *Curr Opin Pharmacol.* 2004;4:189-97.
49. Roland R, Wade J, Davalos M, Nancy R, Jim W, Milagros D. The systemic inflammatory response syndrome in acute liver failure. *Hepatology.* 2000;32:734-9.
50. Goka AKJ, Wendon JA, Willimas R. Fulminant hepatic failure, endogenous endotoxemia, and multiple systems organ failure. In: Matuschack GM, editor. Multiple systems organ failure: hepatic regulation of host defense. New York: Marcel Decker Inc; 1993. p.215-28.
51. Munoz SJ. Difficult management problems in fulminant hepatic failure. *Semin Liver Dis.* 1993;13:395-413.
52. O'Grady JG, Alexander GJM, Mayllar KM, Williams R. Early indicators of prognosis in FHF. *Gastroenterology.* 1989;97:439-45.
53. Anand AC, Nightingale P, Neuberger JM. Early indicators of prognosis in fulminant hepatic failure: an assessment of the King's criteria. *J Hepatol.* 1997;26:62-8.
54. Mitchell I, Bihari D, Chang R. Earlier identification of patients at risk from acetaminophen-induced acute liver failure. *Crit care Med.* 1998;26:279-84.
55. Bernuau J, Goudeau A, Poynard T, Dubois F, Lesage G, Yvonnet B, Degott C, Bezeaud A, Rueff B, Benhamou JP. Multivariate analysis of prognostic factors in fulminant hepatitis B. *Hepatology* 1986;6(4):648-51.
56. Bernau J, Samuel D, Durand Fl. Criteria for emergency liver transplantation with acute viral hepatitis and factor V level 50% of normal: a prospective study [abstract]. *Hepatology.* 1991;14:49A.
57. Lee WM, Galbraith RM, Watt GH. Predicting survival in fulminant hepatic failure using serum-Gc protein concentrations. *Hepatology* 1995;21:101-5.
58. Karvountzis GG, Redecker AG. Relation of alpha-fetoprotein in acute hepatitis to severity of prognosis. *Ann Intern Med.* 1974;80:156-60.
59. Riordan SM, Williams R. Mechanisms of hepatocyte injury, multi-organ failure and prognostic criteria in acute liver failure. *Sem Liver Dis.* 2003;23(3):203-15.
60. Wustrow T, van Hoorn-Hickman R, van Hoorn WA, Fischer A, Terblanche J. Acute hepatic ischemia in the pig: changes in plasma hormones, amino acids and brain biochemistry. *Hepatol Gastroenterol.* 1981;28:143-6.
61. Hazell AS, Butterworth RF. Hepatic encephalopathy: an update of pathophysiologic mechanisms. In: Pathophysiology of Hepatic encephalopathy. *Soc Exp Biol Med.* 1999.222:99-112.
62. Scotto J, Opolon P, Eteve J. Liver biopsy and prognosis in acute liver failure. *Gut.* 1973;14:927-33.
63. Starlz TE, Marchioto T, Kualla K. Homo-transplantation of the liver in humans. *Surg Gynecol Obstet.* 1963;117:659-76.

64. Botha JF, Spearman CW, Millar AJW, Michell L, Gordon P, Lopez T. Ten years of liver transplantation at Groottesuur hospital. *SAMJ*. 2000;90(9):880-3.
65. Millar AJW, Spearman W, McCullogh M, Goddard E, Raad J, Rode H. Liver transplantation for children: the Red Cross Children's hospital experience. *Pediatr Transplant*. 2004;8:136-44.
66. Sauer IM, Goetz M, Steffen I, Walter G, Kahr DC, Schwartlander R. *In vitro* comparison of the Molecular Adsorbent Recirculation System (MARS) and Single-pass Albumin Dialysis (SPAD). *Hepatology*. 2004;39(5):1408-14.
67. Braun KM, Degen JL, Sandgren EP. Hepatocyte transplantation in a model of toxin-induced liver disease: variable therapeutic effect during replacement of damaged parenchyma by donor cells. *Nature Med*. 2000;6:320-6.
68. Chan C, Berthiaume F, Nath BD, Tilles AW, Toner M, Yarmush ML. Hepatic tissue engineering for adjunct and temporary liver support: critical technologies. *Liver Transplant* 2004;10(11):1331-42.
69. Gerlach JC, Seilinger K, Patzer JF. Bioartificial liver systems: Why, what, whither? *Regen Med* 2008;3(4):575-95.
70. Chamuleau RAFM, Poyck PC, van de Kerkhove MP. Bioartificial liver: Its pros and cons. *Ther Apher Dial* 2006;10(2):168-74.
71. Mc Kenzie TJ, Lillegard JB, Nyberg SL. Artificial and bioartificial liver support. *Semin Liver Dis* 2008;28:210-17.
72. Stadlbauer V, Jalan R. Acute liver failure: liver support therapies *Curr Opin Crit Care* 2007;13:215-21.
73. Gerlach JC, Botsch M, Kardassis D. Experimental evaluation of a cell module for hybrid liver support. *Int J Artif Org*. 2001;24:793-8.
74. Ellis AJ, Hughes RD, Wendon JA. Pilot-controlled trial of the extracorporeal liver assist device in acute liver failure. *Hepatology*. 1996;24:1446-51.
75. Demetriou AA, Brown RS, Busutil RW, Fair J, McGuire BM, Rosenthal P, Esch JMA, II, Lerut J, Nyberg SL, Salizzoni M, Fagan EA, de Hemptinne B, Broelsch CE, Muraca M, Salmeron JM, Rabkin JM, Metselaar HJ, Pratt D, De La Mata M, McChesney LP, Everson GT, Lavin PT, Stevens AC, Pitkin Z, Solomon BA. Prospective, Randomized, Multicenter, Controlled Trial of a Bioartificial Liver in Treating Acute Liver Failure. *Ann Surg* 2004;239: 660-70.
76. Xue YL, Zhao SF, Luo Y. TECA hybrid artificial liver support system in treatment of acute liver failure. *World J Gastroenterol*. 2001;7:826-9.
77. Mazariegos GV, Kramer DJ, Lopez RC. Safety observations in phase I clinical evaluation of the Excorp Medical Bio-artificial Liver Support System after the first four patients. *ASAIO*. 2001;47:471-5.
78. Morsiani E, Pazzi P, Puviani AC. Early experiences with a porcine hepatocyte-based bio-artificial liver in acute hepatic failure patients. *Int J Artif Org*. 2002;25:192-202.
79. Sauer IM, Zelinger K, Obermayer N. Primary human liver cells as source for modular extracorporeal liver support-a preliminary report. *Int J Artif Org*. 2002;25:1001-5.
80. van de Kerkhove MP, Di Florio E, Scuderi V. Phase I clinical trial with the AMC-bio-artificial liver. *Int J Artif Org*. 2002;25:950-9.
81. Ding YT, Qiu YD, Chen Z. The development of a new bio-artificial liver and its application in 12 acute liver failure patients. *World J Gastroenterol*. 2003;9:829-32.
82. Streetz K, Bioartificial liver devices- tentative but promising progress. *J Hepatol* 2008;48:189-91.

83. Morsiani E, Brogli M, Galavotti D, Pazzi P, Puviani AC, Azzena GF. Biologic liver support: optimal cell source and mass. *Int J Artif Org.* 2002;25(10):985-93.
84. Tsiaoussis J, Newsome PN, Nelson LJ, Hayes PC, Plevris JN. Which hepatocyte will it be? Hepatocyte choice for bio-artificial liver support systems. *Liver Transpl.* 2001;7(1):2-10.
85. Kobayashi N, Okitsu T, Tanaka N. Cell choice for bio-artificial livers. *Keio J Med* 2003;52(3):151-7.
86. Allen JW, Bhatia SN. Improving the next generation of bio-artificial livers. *Cell Develop Biol.*2002;13:447-54.
87. Nieuwoudt MJ, Kreft E, Olivier B, Malfeld S, Vosloo J, Stegman F, van der Merwe SW. A Large Scale Automated Method for Hepatocyte Isolation: effects on Proliferation in Culture. *Cell Transplant.* 2005;14(5):291-9.
88. Nieuwoudt M, Moolman S, Van Wyk AJ, Kreft E, Olivier B, Laurens JB, Stegman F, Vosloo J, Bond R, van der Merwe SW. Hepatocyte Function in a Radial-flow Bioreactor Using a Perfluorocarbon Oxygen Carrier. *Artif Organs* 2005; 29(11): 915-918.
89. Hansen BA, Poulsen HE. The capacity of urea-N synthesis as a quantitative measure of the functional liver mass in rats. *J Hepatol.* 1986;2:468-74.
90. Eguchi S, Lilja H, Hewitt WR, Middleton Y, Demetriou AA, Rozga J. Loss and recovery of liver regeneration in rats with fulminant hepatic failure. *J Surg Res.* 1997;72:112-22.
91. Sussman NL, Kelly JH. Artificial Liver: a forthcoming attraction. *Hepatology.* 1993;17:1163-4.
92. Allen JW, Hassanein T, Bathia SN. Advances in bio-artificial liver devices. *Hepatology.* 2001;34:447-55.
93. Demetriou AA, Reisner A, Sanchez J. New method of hepatocyte transplantation and extracorporeal liver support. *Ann Surg.* 1986;204:259-71.
94. Moolman FS. Oxygen carriers for a novel bio-artificial liver support system. (dissertation) University of Pretoria, 2004, available at <http://upetd.up.ac.za/etd-09092004-162043>.
95. Rozga J, Morsiani E, Le Page E, Moscioni AD, Giorgio I, Demetriou AA. Isolated hepatocytes in a bio-artificial liver: a single group view and experience. *Biotechnol Bioeng.* 1994;43:645-53.
96. Porter RK, Brand MD. Causes of differences in respiration rate of hepatocytes from mammals of different body mass. In: *Regulatory Integrative Comp Physiol. Am Physiol Soc* 1995;38:R1213-24.
97. Bircher J, Benhamou JP, McIntyre N, Rizzetto M, Rodes J. editors. Physiology of hepatic blood flow. In: Oxford textbook of Clinical Hepatology; 2nd Edition, Oxford University Press: 1999; Chapter 2: p.69-72.
98. McClelland RE, MacDonald J, Coger RN. Modeling O₂ transport within engineered hepatic devices. *Biotechnol Bioeng.* 2003;82(1):12-27.
99. Morsiani E, Galavotti AC, Puviani L, Valieri M, Brogli S, Tosatti S. Radial flow bioreactor outperforms hollow-fiber module as a perfusing culture system for primary porcine hepatocytes. *Transpl Proc.* 2000;32:2715-8.
100. De Bartolo L, Jarosch-Von Schweder G, Haverich A, Bader A. A novel full-scale flat membrane bioreactor utilizing porcine hepatocytes: cell viability and tissue specific functions. *Biotechnol Prog.* 2000;16:102-8.

101. Bader A, De Bartolo L, Haverich A. High level benzodiazepine and ammonia clearance by flat membrane bioreactors with porcine liver cells. *J Biotechnol.* 2000;81:95-105.
102. Morsiani E, Brogli M, Galavotti D, Bellini T, Ricci D, Pazzi P, Puviani AC. Long-term expression of highly differentiated functions by isolated porcine hepatocytes perfused in a radial-flow bioreactor. *Artif Organs.* 2001;25(9):740-8.
103. Yanagi K, Tun T, Taniguchi H, Takada Y, Fukao K, Ohshima N. Development of a packed-bed type bio-artificial liver: metabolic performance of a scaled-up reactor utilizing cultured porcine hepatocytes. *Tissue Eng* 2002:67-73.
104. Flendrig LM, la Soe JW, Jörning GGA, Steenbeck A, Karlsen OT, Bovée WMMJ *et al.* *In vitro* evaluation of a novel bioreactor based on an integral oxygenator and a spirally wound nonwoven polyester matrix for hepatocyte culture as small aggregates. *J Hepatol.* 1997;26:1379-92.
105. Abrahamse SL, van de Kerkhove MP, Sosef MN, Hartman R, Chamuleau RAFM. Treatment of acute liver failure in pigs reduces hepatocyte function in a bio-artificial liver support system. *Int J Artif Org.* 2002;25:966-74.
106. Gerlach JC. Development of a hybrid liver support system: a review. *Int J Artif Org.* 1996;19:645-54.
107. Hay PD, Veitch AR, Gaylor JDS. Oxygen transfer in a convection enhanced hollow fiber bio-artificial liver. *Artif Organs.* 2001;25(2):119-30.
108. Yana IV. *In vivo* synthesis of tissues and organs. In: R Lanza, R Langer, W Chick, editors. Principles of Tissue Engineering, Austin, TX: Landes & Co. 1997. p.169-178.
109. Allen JW, Bhatia SN. Formation of steady-state oxygen gradients *in vitro*. *Biotechnol Bioeng.* 2003;82(3):253-62.
110. Patent: Van Wyk AJ, Bond RP, Moolman FS, van der Merwe SW. Bioreactor device. PCT application WO0222775. (Granted NL 1018924C, EA4455, FR2814468).
111. Van Wyk AJ, Malherbe G, Moolman SF, Nieuwoudt M, van der Merwe SW. Design, development and experimental verification of a novel bioartificial liver support system. *SAGES* 2003. poster and oral presentation.
112. Ronné LJT. Design considerations and analysis of a bioreactor for application in a bioartificial liver support system. (MEng dissertation) University of Pretoria 2007.
113. Puviani AC, Ottolenghi C, Tassinari B, Pazzi P, Morsiani E. An update on high-yield isolation methods and on the potential clinical use of isolated liver cells. *Compar Biochem Physio.* 1998;Part A 121:99-109.
114. Sachs DH. The pig as a potential xenograft donor. *Vet Immunol Immunol pathol.* 1994;58:185-91.
115. Gerlach JC, Brombacher J, Kloppel K, Schnoy N, Neuhaus P. Comparison of four methods for mass hepatocyte isolation from pig and human livers. *Transplantation* 1994;57: 1318-22.
116. Gerlach JC, Brombacher J, Smith M, Neuhaus P. High yield isolation from pig livers for investigation of hybrid liver support systems: Influence of collagenase concentration and body weight. *J Surg Res* 1996;62: 85-9.
117. Seglen, PO. Preparation of rat liver cells. *Methods Cell Biol.* 1976;13:29-34.
118. Morsiani E, Rozga J, Scott HC, Lebow LT, Moscioni AD, Kong LB, Mc Grath MF, Demetriou AA. Automated liver cell processing facilitates large scale isolation and purification of porcine hepatocytes. *ASAIO J.* 1995;41:155-61.

119. Foy BD, Lee J, Morgan J, Toner M, Tompkins RG, Yarmush ML. Optimization of hepatocyte attachment to microcarriers: Importance of oxygen. *Biotech Bioeng* 1993;42:579-88.
120. Nishikawa M, Uchino J, Matsushita M, Takahashi M, Taguchi K, Koike M, Kamachi H, Kon H. Optimal oxygen tension conditions for functioning cultured hepatocytes in vitro. *Artificial Organs*. 1996;20(2):169-77.
121. Rotem A, Toner M, Bhatia S, Foy BD, Tompkins RG, Yarmush ML. Oxygen is a factor determining in vitro tissue assembly: Effects on attachment and spreading of hepatocytes. *Biotech Bioeng*. 1994;43:654-60.
122. Talamini MA, Kappus B, Hubbard A. Repolarization of hepatocytes in culture. *Hepatology*. 1997;25(1):167-72.
123. Falasca L, Michelli A, Sartori E, Tomassini A, Devirgiliis LC. Hepatocytes Entrapped in Alginate Gel Beads and Cultured in Bioreactor: Rapid Repolarization and Reconstitution of Adhesion Areas. *Cells Tissues Organs* 2001;168:126-36.
124. Lecluyse EL, Fix JA, Audus KL, Hochman JH. Regeneration and Maintenance of Bile Canalicular Networks in Collagen-sandwiched Hepatocytes. *Toxicology in Vitro* 2000;14: 117-32.
125. Hoekstra R, Chamuleau RAFM. Recent developments on human cell lines for the bio-artificial liver. *Int J Artif Org*. 2002;25(3):182-91.
126. Smith MD, Smirthwaite AD, Cairns DE, Cousins RB, Gaylor JD. Techniques for measurement of oxygen consumption rates of hepatocytes during attachment and post-attachment. *Int J Artif Org* 1996;19(1):36-44.
127. Sand T, Condie R, Rosenberg A. Metabolic crowding effect in suspension of cultured lymphocytes. *Blood*. 1977;50(2):337-46.
128. Kleiber M. Body size and metabolic rate. *Physiol Rev*. 1947;27:511-41.
129. Wang Z, O'Connor P, Heshka S, Heymsfield SB. The reconstruction of Kleiber's law at the organ-tissue level. *Am Soc Nutrit Sci, Nutritional Methods Res Comm*. 2001:2967-70.
130. Balis UJ, Behnia K, Dwarakanath B, Bhatia SN, Sullivan SJ, Yarmush ML, Toner M. Oxygen consumption characteristics of porcine hepatocytes. *Metabol Eng* 1999;1:49-62.
131. Ju LK, Lee JF, Armiger WB. Enhancing oxygen transfer in bioreactors by perfluorocarbon emulsions. *Biotechnol Prog*. 1991;7:323-9.
132. McMillan JD, Wang DIC. Enhanced oxygen transfer using oil-in-water dispersions. *Ann. New York Acad Sci*. 1987;506:569-82.
133. Elibol M, Mavituna F. Effect of perfluorodecalin as an oxygen carrier on actinorhodin production by *Streptomyces coelicor*. *Appl Microbiol Biotechnol*. 1995;43:206-10.
134. Arias IM, Boyer JL, Chisary FV, Fausto N, Jakoby WB, Schachter D, Shafritz DA (editors). 2001. The liver: Biology and Pathobiology. NY, Lippincott, Williams and Wilkins, Philadelphia, p 3.
135. Jundermann K, Kietzmann T. Zonation of parenchymal and non-parenchymal metabolism in liver. *Annu Rev Nutr* 1996;16:179-260.
136. Jundermann K, Thurman RG. Hepatocyte heterogeneity in the metabolism of carbohydrates. *Enzyme* 1992;46:33-58.
137. Lindros KO. Zonation of cytochrome P450 expression, drug metabolism and toxicity in liver. *Gen Pharmacol* 1997;28:191-6.

138. Runge D, Kohler C, Kostrubsky VE, Jager D, Lehman T, Runge DM, May U, Stolz DB, Strom SC, Fleig WE, Michalopoulos GK. Induction of Cytochrome P450 CYP1A1, CYP1A2, and CYP3A4 but not of CYP2C9, CYP2C19, Multidrug Resistance Associated Protein (MDR-1) by Prototypical Inducers in Human Hepatocytes. *Biochem Biophys Res Comm.* 2000;273:333-41.
139. Wolfe D, Schmidt H, Jungermann K. Short-term modulation of glycogen metabolism, glycolysis and gluconeogenesis by physiological oxygen concentrations in hepatocyte cultures. *Eur J Biochem* 1983;135:405-412.
140. Wolfe D, Jungermann K. Long-term effects of physiological oxygen concentrations on glycolysis and gluconeogenesis in hepatocyte cultures. *Eur J Biochem* 1985;151:299-303.
141. Ohno K, Maier P. Cultured rat hepatocytes adapt their cellular glycolytic activity and adenylate energy status to tissue oxygen tension. *J Cellular Physiol* 1994;160:358-66.
142. Allen JW, Khetani SR, Bhatia SN. In vitro zonation and toxicity in a hepatocyte bioreactor. *Toxicol Sci* 2005;84:110-9.
143. Sivaraman A, Laech JK, Toiwsend S, Iida T, Hogan BJ, Stolz DB, Fry R, Samson LD, Tannenbaum SR, Griffith LG. A microscale in vitro physiological model of the liver: Predictive screens for drug metabolism and enzyme induction. *Curr Drug Metab* 2005;6:569-91.
144. Riccalton-Banks L, Liew C, Bhandari R, Fry J, Shakesheff K. Long-term culture of functional liver tissue: 3-D coculture of primary hepatocytes and stellate cells. *Tissue engineering* 2003;9(3):401-410.
145. Watanabe T, Shibata N, Westerman KA, Okitsu T, Kobayashi N. Establishment of immortalized human hepatic stellate scavenger cells to develop bioartificial livers. *Transplantation* 2003;75:1873-80.
146. Morin O, Normand C. Long-term maintenance of hepatocyte functional activity in co-culture. *J Cellular Physiol* 1986;129:103-10.
147. Okamoto M, Ishida Y, Keogh A, Strain A. Evaluation of the function of primary human hepatocytes co-cultured with the human hepatic stellate cell (HSC) line L190. *Int J Artif Org* 1998;6:353-9.
148. Lowe KC, Davey MR, Power JB. Perfluorochemicals: their applications and benefits to cell culture. *Tibtech* 1998;16:272-77.
149. King AT, Mulligan BJ, Lowe KC. Review: Perfluorochemicals and cell culture. *Biotechnology* 1989;7:1037-42.
150. Lowe KC, Anthony P, Wardrop J, Davey MR, Power JB. Perfluorochemicals and cell biotechnology. *Art cells, blood subs, immob biotech* 1997;25(3):261-274.
151. Lowe KC. Review. Engineering blood: Synthetic substitutes from fluorinated compounds. *Tissue Engineering* 2003;9(3):389-99.
152. Niu M, Clemens MG, Cogger RN. Optimizing normoxic conditions in liver devices using enhanced gel matrices. *Biotechnol Bioeng* 2007;99(6):1502-12.
153. Khattak SF, Chin K, Bhatia SR, Roberts SC. Enhancing O₂ tension and cellular function in alginate cell encapsulation devices through the use of perfluorocarbons. *Biotechnol Bioeng* 2007;96(1):156-66.
154. Ju LK, Lee JF, Armiger WB. Enhancing oxygen transfer in bioreactors by perfluorocarbon emulsions. *Biotechnol Prog.* 1991;7:323-9.
155. Block GD, Locker J, Bowen WC, Petersen BE, Katyal S, Strom SC, Riley T, Howard TA, Michalopoulos GK. Population expansion, clonal growth and specific

- differentiation patterns in primary cultures induced by HGF/SF, EGF and TDF in a chemically defined (HGM) medium *J Cell Biology* 1996;132(6):1133-49.
156. Runge DM, Runge D, Dorko K, Pisarov LA, Leckel K, Kostrubsky VE, Thomas D, Strom SC, Michalopoulos GK. EGF and HGF activity in serum-free cultures of human hepatocytes. *J Hepatol* 1999;30:265-74.
 157. Su T, Waxman D. Impact of DMSO and expression of nuclear receptors and drug-inducible cytochromes P450 in primary rat hepatocytes. *Arch Biochem Biophys* 2004;424:226-234.
 158. Powers MJ, Janigian DM, Wack KE, Baker CS, Stolz DB, Griffith LG. Functional behaviour of primary rat liver cells in a 3D perfused microarray bioreactor. *Tissue Engineering* 2002;8(3):499-513.
 159. Jasmund I, Schwientek S, Acikgoz A, Langsch A, Machens HG, Bader A. The influence of medium composition and matrix on long-term cultivation of primary porcine and human hepatocytes. *Biomolecular Eng* 2007;24:59-69.
 160. Niuy M, Clemens MG, Cogger RN. Optimizing normoxic conditions in liver devices using enhanced gel matrices. *Biotechnol Bioeng* 2007;99(6):1502-12.
 161. Khattak SF, Chin K, Bhatia SR, Roberts SC. Enhancing O₂ tension and cellular function in alginate cell encapsulation devices through the use of perfluorocarbons. *Biotechnol Bioeng* 2007;96(1):156-66.
 162. Sullivan J, Harris DR, Palmer AF. Convection and hemoglobin-based O₂ carrier enhanced transport in a HF bioreactor. *Artif Cells, Bl Subs, Biotechnol* 2008;36:386-402.
 163. Mareels G, Poyck P, Elloot S, Chamuleau R, Verdonck P. Numerical simulation of fluid flow and oxygen transport in a full scale model of the AMC Bioartificial liver with an in vitro determined hepatocyte distribution. *Ann Biomed Eng.* 2006 34(11):1729-44.
 164. Freire MG, Dias AMA, Coutinho JAP, Coelho MAZ, Marrucho IM. Enzymatic method for determining O₂ solubility in perfluorocarbon emulsions. *Fluid Phase Equilibria* 2005;231:109-13.
 165. Martin Y, Vermette P. Bioreactors for tissue mass culture: Design, characterisation and recent advances. *Biomaterials* 2005;26:7481-503.
 166. Heath CA, Hammer BE, Pimbley JM. Magnetic resonance imaging of flow in HF bioreactors. *AIChE J* 1990;36(4):547-58.
 167. Donoghue C, Brideau M, Newcomer P, Pangrle B, DiBasio D, Walsh E, Moore S. Use of MRI to analyse the performance of HF bioreactors. *Ann NY Acad Sci* 1992;665:285-300.
 168. Planchamp C, Ivancevic MK, Pastor CM, Valle'e JP, Pochon S, Terrier F, Mayer JM, Reist M. Hollow Fiber Bioreactor: New Development for the Study of Contrast Agent Transport Into Hepatocytes by Magnetic Resonance Imaging. *Biotechnol Bioeng* 2004;85(6):656-65.
 169. Ferreira EC, Mota M, Pons MN. Image analysis and multiphase bioreactors Chptr 2 in Multiphase Bioreactor design, JMS Cabral, M Mota, J Tramper (eds) Taylor & Francis, London 25-52, 2001.
 170. Kofidis T, Lenz A, Boublik J, Akhyari P, Wachsmann B, Stahl KM, Haverich A, Leyh RG. Bioartificial grafts for transmural myocardial restoration: a new cardiovascular tissue culture concept. *Eur J Cardio-thoracic Surg* 2003;24:906-11.
 171. Kofidis T, Lenz A, Boublik J, Akhyari P, Wachsmann B, Stahl KM, Hofmann M, Haverich A. *Biomaterials* 2003;24:5009-14.

172. Walles T, Giere B, Hofmann M, Schanz J, Hofmann F, Mertsching H, Macchiarini P. Experimental generation of a tissue-engineered functional and vascularized trachea. *Gen Thoracic Surg* 2004;129(6):900-6.
173. Phelps ME. Positron emission tomography provides molecular imaging of biological processes. *PNAS* 2000;97(16):9226-33.
174. Mc Kenzie TJ, Lillegard JB, Nyberg SL. Artificial and bioartificial liver support. *Semin Liver Dis* 2008;28:210-17.
175. Fishman JA, Patience C. Xenotransplantation: Infectious risk revisited. *Amer J Transplant* 2004;4:1383-90.
176. Sprangers B, Waer M, Billiau AD. Xenotransplantation: Where are we in 2008? *Kidney International* 2008;74:14-21.
177. Wilhelm M, Fishman JA, Pontikis R, Aubertin AM, Wilhelm FX. Susceptibility of recombinant PERV reverse transcriptase to nucleoside and non nucleoside inhibitors. *Cell Mol Life Sci* 2002;59:2184-90.
178. Ramsoondar J. Conference abstract. *Xenotransplantation* 2007;14:400.
179. Phelps CJ, Koike C, Vaught TD. Production of α 1,3 galactosyltransferase deficient pigs. *Science* 2003;299:411-14.
180. Miyagawa S, Nakatsu S, Nakagawa T, Kondo A, Matsunami K, Hazama et al. Prevention of PERV infections in pig to human xenotransplantation by the RNA interference silences gene. *J Biochem* 2005;137:503-8.
181. Cooper DKC, Ezzelrahab M, Hara H, Ayares D. Recent advances in pig-to-human organ and cell transplantation. *Expert Opin Biol Ther* 2008;8(1):1-4.
182. Dwyer KM, Robson SC, Nandukar HH. Thromboregulatory manifestations in human CD39 transgenic mice and the implications for thrombotic disease and transplantation *J Clin Invest* 2004;113:1440-6.
183. Chen D, Weber M, McVey JH. Complete inhibition of acute humoral rejection sing regulated expression of membrane-tethered anticoagulants on xenograft endothelium *Am J Transplant* 2004;4:1958-63.
184. Cozzi E, White DJ. The generation of transgenic pigs as potential organ donors for humans. *Nat Med* 1995;1:964-6.
185. Hara H, Long C, Lin YJ, Tai HC, Ezzelrahab M, Ayares D, Cooper DKC. *In vitro* investigation of pig cells for resistance to human antibody-mediated rejection. *Transplant Int* 2008. not yet published. doi:10.1111/j.1432-2277.2008.00736.x
186. Sandgren EP, Palmiter RD, Heckel JL. Complete hepatic regeneration after somatic deletion of an albumin activator transgene *Cell* 1991;66:245-56.
187. Tatenno C, Yoshizane Y, Saito N. Near completely humanized liver in mice shows human-type metabolic responses to drugs *Am J Pathol* 2004;2004:165:901-12.
188. Azuma H, Paulk N, Ranabe A. Robust expansion of human hepatocytes in $Fah^{-/-}/Rag^{2-/-}/Il2rg^{-/-}$ mice. *Nat Biotechnol* 2007;25:903-10.
189. Bissig KD, Le TT, Woods BN, Verma IM. Repopulation of adult and neonatal mice with human hepatocytes: A chimeric animal model *PNAS* 2007;104(51):20507-11.
190. Mavri-Damelin D, Damelin LH, Eaton S, Rees M, Selden C, Hodgson HJF. Cells for bioartificial liver devices: The human hepatoma-derived cell line C3A produces urea but does not detoxify ammonia. *Biotechnol Bioeng* 2007;99(3):644-51.
191. Choi YS, Lee DY, Kim IY, Kang S, Ahn K, Kim HJ. Ammonia removal using hepatoma cells in mammalian cell cultures *Biotechnol Prog* 2000;16(5):760-68.
192. Lorenzini S, Gito S, Grandini E, Andreone P, Bernardi M. Stem cells for end-stage liver disease: How far have we got? *World J Gastroenterol* 2008;14(29):4593-9.

193. Poyck PC, van Wijk ACWA, van der Hoeven TV, de Waart DR, Chamuleau RAFM, van Gulik TM, Oude Elferink RPJ, Hoekstra R. Evaluation of a new immortalized fetal liver cell line (cBAL111) for application in a bioartificial liver. *J Hepatol* 2007; 48(2):266-75.
194. Poyck PC, Hoekstra R, Maas MAW, van Wijk ACWA, van Gulik TM, Chamuleau RAFM. Evaluation of a novel human fetal liver cell line cBAL11 in the AMC-BAL in rats with complete liver ischemia. In Poyck PC PhD thesis: Towards the application of a human liver cell line in the AMC bioartificial liver 2007 ISBN 978-90-9022050-5.
195. Talbot NC, Caperna TJ, Lebow LT, Moscioni D, Pursel VG, Rexroad CE. Ultrastructure, enzymatic and transport properties of the PICM-19 liver cell line. *Exp Cell Res* 1996;225:22-34.
196. Talbot NC, Caperna TJ, Wells KD. The PICM-19 cell line as an in vitro model of liver bile ductules: Effects of cAMP inducers, biopeptides and pH. *Cells, Tissues Organs* 2002;171:99-116.
197. Press release: HepaLife's bioartificial liver exceeds expectations in new tests conducted over prolonged periods of time. May 12, 2008. (www.hepalife.com).
198. Puhl G, Frank J, Muller AR, Steinmuller T, Denner J, Neuhaus P, Gerlach JC. Clinical extracorporeal hybrid liver support- phase I study with primary porcine cells. *Xenotransplantation* 2003;10(5):460-9.
199. Hepalife Inc. Material purchase agreement October 01, 2008 (www.secinfo/d12Pk6.tm8e.htm).
200. Riess JG. Perfluorocarbon-based oxygen delivery. *Artif Cells, Bl subs, Biotechnol* 2006;34:567-80.
201. Krafft MP, Riess JG. Perfluorocarbons: Life Sciences and Medical uses. *J Polym Sci Part A: Polym Chem* 2007;45:1185-98.
202. Spahn DR, Kocian R. The place of artificial oxygen carriers in reducing allogenic blood transfusions and augmenting tissue oxygenation. *Canadian Jnl Anaesthesia* 2003;50(6):41-7.
203. Kim HW, Greenburg AG. Toward 21st century blood component replacement therapeutics: Artificial O₂ carriers *Artif Cells, Bl subs, Biotechnol* 2006;34:537-50.
204. Kuznetsova IN. Perfluorocarbon emulsions: Stability *in vitro* and *in vivo*. *Pharm Chem Jnl* 2003;37(8):415-20.
205. Ingram DA, Forman MB, Murray JJ. Activation of complement by Fluosol attributable to the pluronic detergent micelle structure. *J Cardiovasc Pharmacol* 1993;22:456-61.
206. Noveck RJ, Shanon EJ, Leese PT et al Randomized safety studies of IV perflubron emulsion. II Effects on Immune Function in healthy volunteers. *Anesth Analg* 2000;91:812-22.
207. Noveck RJ, Shanon EJ, Shor JS et al Randomized safety studies of IV perflubron emulsion. I Effects on Coagulation Function in healthy volunteers. *Anesth Analg* 2000;91:804-11.
208. Burgan AR, Herrick WC, Long DM et al. Acute and subacute toxicity of 100% PFOB emulsion. *Biomat Art Cells Art Org* 1988;16(1-3):681-2.
209. Sedova LA, Kochetygov NI, Berkos MV et al. Side reaction caused by the PFC emulsions in IV infusion to experimental animals. *Art Cells, Blood Subs Immob Biotech* 1998; 26(2):149-57.

210. Sloviter HA, Yamada H, Ogoshi S. Some effects of IV administered dispersed fluorochemicals in animals. *Federation Proceedings* 1970;29(5):1755-7.
211. Mattrey RF, Hilpert PL, Long CD. Hemodynamic effects of IV lecithin-based PFC emulsions in dogs. *Crit care Med* 1989;17(7):652-6.
212. Peck W, Mattrey RF, Slutsky RA. Perfluorooctyl bromide: acute hemodynamic effects in pigs of IV administration compared with standard ionic contrast media. *Investigative Radiology* 1984;2:129-32.
213. Nieuwoudt M, Kunneke R, Smuts M, Becker J, Stegmann GF, Van der Walt C, Nester J, Van der Merwe S. Standardization criteria for an ischemic surgical model of acute hepatic failure in pigs. *Biomaterials* 2006; 27(20):3836-45.
214. Higgins GM, Anderson RM. Experimental pathology of the liver. *Arch Pathol* 1931;12:186-202.
215. Emond J, Capron-Laudereau M, Meriggi F, Bernau J, Reynes M, Houssin D. Extent of hepatectomy in the rat. *Eur Surg Res* 1989;21:251-59.
216. Kubota T, Takabe K, Yang M, Sekido H, Endo I, Ichikawa Y. Minimum sizes for remnant and transplanted livers in rats. *J Hep Bil Pancr Surg* 1997;4:398-404.
217. Topaglu S, Izci E, Ozel H, Topaglu E, Avsar F, Saygun O. Effects of TVE application during 70 % hepatectomy on regeneration capacity of rats. *J Surg Res* 2005;124:139-45.
218. Ijichi H, Taketomi A, Yoshizumi T, Uchiyama H, Yonemura Y, Soejima Y. Hyperbaric oxygen induces endothelial growth factor and reduces liver injury in regenerating rat liver after partial hepatectomy. *J Hepatol* 2006;45:28-34.
219. Urakami H, Abe Y, Grisham MB. Role of reactive metabolites of oxygen and nitrogen in partial liver transplantation. *Clin Exp Pharmacol Physiol* 2007;34:912-9.
220. Van de Kerkhove MP, Hoekstra R, van Gulik TM, Chamuleau R. Large animal models of fulminant hepatic failure in artificial and Bioartificial liver support research. *Biomaterials* 2004; 25:1613-25.
221. Seleverstov O, Bader A. Evaluation of liver support systems for preclinical testing by animal trials. *Artificial Organs* 2006;30(10):815-21.
222. Nyberg SL. Galactosamine induced fulminant hepatic failure. *Hepatology*. 1997;26:1367-69.
223. Kalpana K, Ong HS, Soo K.C, Tan SY, Prema Raj J. An improved model of galactosamine induced fulminant hepatic failure in the pig. *J Surg Res*. 1999;82(2):121-130.
224. Grosse H, Ozler Y, Fabre M, Cheruau B, Abbas A, Urbani L. Acetaminophen induced fulminant hepatic failure in pigs: a new model to assess pre-clinical liver assistance (abstract) *Hepatology*. 1996;24:722A.
225. Henne-Bruns D, Artwohl J, Broelsch C, Kremer B. Acetaminophen induced acute hepatic failure in pigs: controversial results to other animals. *Res Exp Med*. (Berlin) 1988;188(6):463-472.
226. Hickman R, Dent DM, Terblanche J. The anhepatic model in a pig. *SAMJ*. 1974;48:263-274.
227. Fournau I, Pirenne J, Roskams T, Yap SH. An improved model of acute liver failure based on transient ischemia of the liver. *Arch Surg*. 2000;135:1183-9.
228. Flendrig LM, Calise F, Di Florio E, Mancini A, Ceriello A. Significantly improved survival time in pigs with complete liver ischemia treated with a novel bio-artificial liver. *Int J Artif Org*. 1999;22:701-708.

229. Ytrebo LM, Nedredal GI, Langbakk B, Revhaug A. An experimental large animal model for the assessment of bio-artificial liver support systems in fulminant hepatic failure. *Scand J Gastroenterol.* 2002;9:1077-88.
230. Newsome PN, Plevris JN, Nelson LJ, Hayes PC. Animal models of fulminant hepatic failure: a critical evaluation. *Liver Transpl.* 2000;6(1):21-31.
231. Terblanche J, Hickman R. Animal models of fulminant hepatic failure. *Dig Dis Sci.* 1991;36:770-4.
232. Rahman TM, Hodgson HJF. Animal models of acute hepatic failure. *Int J Exp Path.* 2000;81:145-57.
233. Bhatnagar A, Majumdar S. Animal models of hepatic encephalopathy. *Ind Soc Gastroenterol.* 2003;22:S33-6.
234. Blei AT, Olafsson S, Webster S, Levy R. Complications of intracranial pressure monitoring in fulminant hepatic failure. *Lancet.* 1993;341:157-8.
235. Chem S, Hewitt W, Demetriou A, Rozga J. Prolonged survival in anhepatic pigs treated with a bioartificial liver. *Surg forum Alimentary tract* 1996;161-3.
236. Hickman R, Bracher M, Tyler M, Lotz Z, Fourie J. Effect of total hepatectomy on coagulation and glucose homeostasis in the pig. *Dig Dis Sci.* 1992;37(3):328-34.
237. Vistoli F, Boggi U, Filliponi F, Mosca F. A standardized pig model of total hepatectomy for testing liver support systems. *Transplant proc* 2000;32:2723-5.
238. Engelbrecht G, Hickman R, Kahn D. One-stage total hepatectomy in the rat using microvascular anastomoses. *Microsurgery* 1999; 19:95-7.
239. Bhatia V, Singh R, Acharya SK. Predictive value of arterial ammonia for complications and outcome in acute liver failure. *Gut* 2006;55:98-104.
240. Clemmesen JO, Larsen FS, Kondrup J, Adel Hansen B, Ott P. Cerebral herniation in patients with acute liver failure is correlated with arterial ammonia concentration. *Hepatology* 1999;29:648-53.
241. Bernal W, Hall C, Karvellas CJ, Auzinger G, Sizer E, Wendon J. Arterial ammonia and clinical risk factors for encephalopathy and intracranial hypertension in acute liver failure. *Hepatology* 2007;46(6):1844-52.
242. Sauer IM, Neuhaus P, Gerlach JC. Concept for modular extracorporeal liver support for the treatment of acute hepatic failure. *Metab Brain Dis* 2002;17(4):477-84.
243. Lee W, Squires RH, Nyberg SL, Doo E, Hoofnagle JH. Acute liver failure: Summary of a workshop. Meeting report. *Hepatology* 2008;47(4):1401-15.
244. Cruz D, Bellomo R, Kellum JA, de Cal M, Ronco C. The future of extracorporeal support. *Crit Care Med* 2008;36(4):S243-52.
245. Evenepoel P, Laleman W, Wilmer A, Claes K, Kuypers D, Bammens B, Nevens F, Vanreberghem Y. Prometheus versus MARS: Comparison of efficiency in two different liver detoxification devices. *Artif Org* 2006;30(4):276-84.
246. Ferenci P, Kramer L. MARS and the failing liver- any help from the outer space? *Hepatology* 2007;46(6):1682-4.
247. Sauer IM, Goetz M, Steffen I, Walter G, Kehr DC, Schwartlander R, Hwang YJ, Pascher A, Gerlach JC, Neuhaus P. In vitro comparison of the MARS and SPAD. *Hepatology* 2004;39:1408-14.
248. Rozga J, Umehara Y, Trofimenko A, Sadahiro T, Demetriou AA. A novel plasma filtration therapy for hepatic failure: preclinical studies. *Ther Apher Dial* 2006;10(2):138-144.
249. Ho DW, Fan ST, To J. Selective plasma filtration for treatment of FHF induced by galactosamine in a pig model. *Gut* 2002; 50:869-76.

250. Rowland M, Tozer TN. Clinical pharmacokinetics concepts and applications. Philadelphia; Lea and Febinger. 1989.
251. Iwata H, Ueda Y. Pharmacokinetic considerations in the development of a bio-artificial liver. *Clin Pharmacokinet*. 2004; 43(4):211-25.
252. Park YG, Iwata H, Ikada Y. Derivation of pharmacokinetics equations for quantitative evaluation of bio-artificial liver functions. *Ann NY Acad Sci*. 2001;944:296-307.
253. Iwata H, Park YG, Ikada Y. Importance of the extracorporeal circulation rate in a bio-artificial liver. *Material Sci Eng*. 1998;C6:235-43.
254. Catapano G, de Bartolo L. Importance of the kinetic characterization of liver cell metabolic reactions to the design of hybrid liver support devices. *Int Jnl Artif Org*. 1996;19(1):670-6.
255. Kanamori T, Yanagi K, Sato T, Shinbo T, Ohshima N. System design of a bio-artificial liver with a high performance hemodialyzer as an immunoisolator using a mathematical kinetic model. *Int J Artif Org*. 2003;26(4):308-18.
256. Ohshima N, Shiota M, Kusano H, Wada G, Tsunetsugu T, Ookawa K, Yanagi K. Kinetic analyses of the performances of a hybrid-type artificial liver support system utilizing isolated hepatocytes. *Material Sci Eng* 1994;C1:79-85.
257. Park YG, Son YS, Ryu HW. Perfusion model for detoxification of drugs in a bio-artificial liver. *Int Jnl Artif Org* 2003;26(5):383-94.
258. Palmes D, Spegel HU. Animal models of liver regeneration. *Biomaterials*. 2004;25:1601-11.
259. Jakubowski A, Ambrose C, Parr M, Lincecum JM, Wand MZ. TWEAK induces liver progenitor cell proliferation. *J Clin Invest*. 2005; 115:2330-40. doi:10.1172/JCI23486.
260. Bailey B, Amre DK, Gaudreault P. Fulminant hepatic failure secondary to acetaminophen poisoning: A systematic review of prognostic criteria. *Crit Care Med* 2003;31(1):299-305.
261. Choi WC, Arnaout WC, Villamil FG, Demetriou AA, Vierling JM. Comparison of the applicability of two prognostic scoring systems in patients with fulminant hepatic failure. *Korean J Int Med* 2007;22:93-100.
262. Kamath PS, Wiesner RH, Malinchoc M, Kremers W, Therneau TM, Kosberg CL, D'Amico G, Dickson ER, Kim WR. A model to predict survival in patients with end-stage liver disease. *Hepatology* 2001;33:464-70.
263. Pelaez-Luna M, Martinex-Salgado J, Olivera-Martinez MA. Utility of the MAYO end-stage liver disease score, King's college criteria and a new in-hospital mortality score in the prognosis of in-hospital mortality in acute liver failure. *Transplant Proc* 2006;38:927-9.
264. Ripoll C, Banares R, Rincon D, Catalina MV, Iacono OL, Salcedo M, Clemente G, Nunez O, Matilla A, Molinero LM. Child, MELD, hyponatremia and now portal pressure. *Hepatology* 2005;42:793-801.
265. Huo TI, Lin HC, Wu JC, Lee FY, Hou MC, Lee PC, Chang FY, Lee SD. Proposal of a modified Child-Turcotte-Pugh scoring system and comparison with the MELD for outcome prediction in patients with cirrhosis. *Liver Transplantation* 2006;12:65-71.
266. Cholongitas E, Senzolo M, Patch D, Kwong K, Nikolopoulou V, Leandro G, Shaw S, Burroughs AK. Risk factors, SOFA and MELD scores for predicting short term mortality in cirrhotic patients admitted to intensive care unit. *Aliment Pharmacol Ther* 2006;23:883-93.

267. Dabos JD, Newsome PN, Parkinson JA, Davidson JS, Sadler IH, Plevris JN, Hayes PC. A biochemical prognostic model of outcome in paracetamol-induced acute liver injury. *Transplantation* 2005;80(12):1712-6.
268. Bernal W, Donaldson N, Wyncoll D, Wendon J. Blood lactate as an early predictor of outcome in paracetamol-induced acute liver failure: a cohort study. *Lancet* 2002;359:558-63.
269. Novelli G, Rossi M, Pugliese F, Poli I, Ruberto E, Martelli S, Nudo F, Morabito V, Mennini G, Berloco PB. Molecular adsorbents recirculating system treatment in acute-on-chronic hepatitis patients on the transplant waiting list improves model for end stage liver disease scores. *Transplant Proc* 2007;39:1864-7.
270. For example see YSI 7100 multi parameter bio-analytical system, www.YSI.com 2007.
271. For example see CMA 600 multi parameter clinical microdialysis system, www.microdialysis.se
272. Booch G, Jacobsen I, Rumbaugh J. OMG Unified Modeling Language Specification, available online, www.uml.org, 2008.
273. Aggarwal V. The application of the unified modeling language in object-oriented analysis of healthcare information systems. *J Med Syst*, 2002; 26(5): 383-97.
274. Xiao-Lang X, Wang L, Zhou H. A UML profile for framework modeling. *J Zhejiang Univ Sci*, 2004; 5(1): 92-8.
275. Van der Maas AF, ter Hofstede A, ten Hoopen AJ. Requirements for medical modeling languages. *J Am Med Inform Assoc*, 2001; 8: 146-62.
276. Roux-Rouquié M, Caritey N, Gaubert L, Le Grand B, Soto M. Metamodel and modeling language: Towards a unified modeling language (UML) profile for systems biology. *T Comp Sys Biology* 2005; in press.
277. Roux-Rouquié M, Soto M. Virtualization in *Systems Biology: Metamodels* and modeling languages for semantic integration. *T Comp Sys Biology* 2005;(1):28-43.
278. Roux-Rouquié, M., Caritey, N., Gaubert, L. *Using the Unified Modelling Language (UML) to guide the systemic description of biological processes and systems.* *Biosystems* 2004;75:3-14.
279. van der Heijden RTJM, Hellinga C, Lutben K, Honderd G. State estimators (observers) for the on-line estimation of non-measurable process variables. *Tibtech* 1989; 7: 205-9.
280. Leleux DP, Claps R, Chen W, Tottel FK, Harman TL. Applications of Kalman filtering to real-time trace gas concentration measurements. *Appl Phys* 2002;B74:85-93.
281. Simutis R, Havlik I, Lubbert A. A fuzzy-supported extended Kalman filter. *J Biotechnol* 1992;24:211-34
282. Stephanopoulos G, Park S. Bioreactor state estimation. in *Biotechnology* 2nd edition, Volume 4 Measuring Modeling and Control, VCH Verlagsgesellschaft mbH, Weinheim Germany 1991.
283. Pelletier F, Fonteix C, da Silva AL, Marc A, Engasser JM. Software sensors for monitoring perfusion cultures: Evaluation of the hybridoma density and the medium composition from glucose concentration measurements. *Cytotechnology* 1994; 15: 291-9.
284. Sprent P. *Data-driven statistical modeling.* London, Chapman and Hall, Thompson Science, 1998.

285. Myerson RB. Probability Models for Economic Decisions. University of Chicago, Chicago, Thomson/Brooks/Cole, 2005.
286. Hogg RV, Craig AT. Introduction to Mathematical Statistics, 5th ed, New York, Macmillan, 1995.
287. Landau DP, Binder K. A guide to Monte Carlo analysis in statistical physics. 2nd edition, Cambridge University Press. 2005.
288. Wendon J. What to monitor and why? *EASL congress Copenhagen 2007*.
289. Kramer DJ. Prevention and management of infections and MOF. *EASL congress Copenhagen 2007*.
290. Finney RL, Thomas GB editors. Calculus, Reading Massachusetts, Addison-Wesley, 1990, Section 9.7. p.623-44.
291. Hanson CW, Marshall BE. Artificial intelligence applications in the intensive care unit. *Crit Care Med* 2001; 29(2): 427-35.
292. Raghavan SR, Ladik V, Meyer KB. Developing decision support for dialysis treatment of chronic kidney failure. *IEEE Trans Inf Tech Biomed* 2005; 9(2): 229-38.
293. Jeanpierre L, Charpillat F. Automated medical diagnosis with fuzzy stochastic models: Monitoring chronic diseases. *Acta Biotheoretica* 2004; 52: 291-311.
294. Mahfouf M, Abbod MF, Linkens DA. A survey of fuzzy logic monitoring and control utilization in medicine. *Artif Intell Med* 2001; 21: 27-42.
295. Toma T, Abu-Hanna A, Bosman RJ. Discovery and integration of univariate patterns from daily individual organ-failure scores for intensive care mortality prediction. *Artif Intell Med*. 2008;43(1):47-60.
296. Toma T, Abu-Hanna A, Bosman RJ. Discovery and inclusion of SOFA score episodes in mortality prediction. *J Biomed Inform*. 2007;40(6):649-60.
297. Romsa P, Heikkinen J, Biancari F, Pokela M, Rimpilainen J, Vainionpaa V. Prolonged hypothermia after experimental hypothermic circulatory arrest in a chronic porcine model. *J Thorac Cardiovasc Surg*. 2002;123:724-34.
298. Takada Y, Ishiguro S, Fukunaga K, Gu M, Taniguchi H, Seino K. Increased intracranial pressure in a porcine model of fulminant hepatic failure using amatoxin and endotoxin. *J Hepatol*. 2001;34:825-31.
299. Hanid MA, Mackenzie RL, Jenner RE, Chase RA, Mellon PJ, Trewby PN. Intracranial pressure in pigs with surgically induced acute liver failure. *Gastroenterology* 1979;76(1):123-31.
300. Cimander C, Carlsson M, Mandenius CF. Sensor fusion for *on-line* monitoring of yoghurt fermentations. *J Biotechnol*. 2002;99:237-48.
301. Dowd JE, Weber I, Rodriguez B, Piret JM, Kwok KE. Predictive control of hollow-fiber bioreactors for the production of monoclonal antibodies. *Biotechnol Bioeng* 1999;63(4):484-92.
302. Kovarova-Kova K, Gehlen S, Kunze A, Keller T, von Daniken R, Kolb M, van Loon A. Application of model-predictive control based on artificial neural networks to optimize the fed-batch process for riboflavin production. *J Biotechnol* 2000;78:39-52.
303. Hoffman F, Schmidt M, Rinas U. Simple technique for simultaneous *on-line* estimation of biomass and acetate from base consumption and conductivity measurements in high-cell density cultures of *Escherichia coli*. *Biotechnol Bioeng* 2000;70:358-61.
304. Erlenkotter A, Fobker M, Chemnitz GC. Biosensors and flow-through system for the determination of creatinine in hemodialysate. *Anal Bioanal Chem* 2002; 372: 284-92.

305. Lindberg LS, Ask P, Fridolin I, Magnusson M, Uhlin F, Ragnemalm B. Sensors for non-invasive regulation of dialysis. Linkopings University, Sweden, available at <http://www.imt.liu.se/fmtpa/research/dialysis.html>, accessed November 2005.
306. Harms P, Kostov Y, Tao G. Bioprocess monitoring. *Curr Opin Biotechnol.* 2002;13:124-27.
307. Pijanowska DG, Dawgul M, Torbicz W. Comparison of urea determination in biological samples by Enfets on pH and pNH₄ detection. *Sensors.* 2003;3:160-65.
308. Ulber R, Frerichs JG, Beutel S. Optical sensor systems for bioprocess monitoring. *Anal Bioanal Chem.* 2003;376:342-48.
309. Lenz R, Kuhn KA. Towards a continuous evolution and adaptation of information systems in medicine. *Int J Med Informatics.* 2004;73:75-89.
310. Wilcox A, Hripcsak G, Chen C. Creating an environment for linking knowledge-based systems to a clinical database: a suite of tools. *AMIA.* 1997:303-7.
311. Schugerl K, Progress in monitoring, modeling and control of bioprocesses during the last 20 years. *J Biotechnol.* 2001;85:149-73.
312. Buntmeyer H, Marzahl Rand J, Lehmann J, A direct control concept for mammalian cell fermentation processes. *Cytotechnol.* 1994;15:271-9.
313. Roger JM, Sablayrolles JM, Steyer JP, Bellon-Maurel V. Pattern analysis techniques for process fermentation curves. *Biotechnol Bioeng.* 2002;79(7):804-15.
314. Palfreyman N. The construction of meaning in computational and integrative biology. *Jnl Integrative Biol.* 2004;8(2):95-105.
315. Belforte G, Bona B, Milanese M. Advanced modeling and identification techniques for metabolic processes. *Crit Rev Biomed Eng.* 1983;10(4):275-316.
316. Brandon EFA, Raap CD, Meijerman I, Beijnen JH, Schellens JHM. An update on *in vitro* test methods in human hepatic drug biotransformation research: pros and cons. *Toxicol Appl Pharmacol.* 2003;189:233-46.
317. Harms P, Kostov Y, Tao G. Bioprocess monitoring. *Curr Opin Biotechnol.* 2002;13:124-27.
318. Freeman RB, Jamieson N, Schaubel DE, Porte RJ, Villamil FG. Who should get a liver graft? *J Hepatol* 2009;50:664-73.

9. APPENDICES

Appendix A: *In vitro* study methods

A.1 Media and chemicals

Minimum essential medium (MEM), Dulbecco's modified Eagle's medium (DMEM) (both with EBSS and L-glutamine) supplemented with fetal bovine serum (FCS) (10% vol/vol) and penstrep fungizone 100X (1% vol/vol) were purchased from Bio-Whittaker, Adcock Ingram Scientific, Johannesburg, South Africa. Gentamycin sulphate ((50 mg/ml at 0.1% vol/vol), Phenix, South Africa), insulin ((I2767) 50 mU/L), glucagon ((G664) 16 µg/L), dexamethasone ((D4902) 67 µg/L) and epidermal growth factor (EGF (E9644) 20µg/L); from Sigma-Aldrich, Johannesburg, South Africa, were added to all media. Filter-sterilized collagenase type IV (Sigma (C5138)) was dissolved in MEM (0.68 g/425 ml) with 0.65 g CaCl₂, 25 ml of FCS and antibiotics as above. Collagenase solution was prepared fresh on the day of the isolation procedure. Washing buffer at 10-15°C contained deionised water with 5% FCS, dexamethasone as above, 7.01 g/L NaCl, 0.46 g/L KCl, 0.10 g/L Ca Cl₂ and 2.383 g HEPES. Perfusion buffer at 37 °C contained 5% FCS, dexamethasone, 9 g/L NaCl, 0.42 g/L KCl, 2.1 g/L NaHCO₃, 0.9 g/L D-Glucose and 4.77 g/L HEPES. For chelation, EDTA (0.58 g/L) was added to Perfusion buffer on the day of the procedure. All buffers were oxygenated with a carbogen gas mixture (5% CO₂ and 90%O₂) during the isolation procedure. Percoll (Sigma (P16440)) was mixed 9:1 with 10X Hank's balanced salt solution (HBSS) (80g/L NaCl, 4g/L KCl, 1/Lg MgSO₄, 0.6g/L KH₂PO₄, 0.4g/L Na₂HPO₄ and 10g of Glucose). Solutions used for perfusing the liver during hepatectomy and transport were, firstly, 1L of clinical saline at 5-10°C, supplemented with 0.58g EDTA, 40mU Insulin, 67 µg/L Dexamethasone and antibiotics, followed by 1L of University of Wisconsin (UW) solution at 5-10 °C, with insulin, dexamethasone and antibiotics. The pH of all solutions was adjusted in a sterile manner to between 7.35 and 7.4 using concentrated HCl or NaOH. insulin, glucagon, dexamethasone and EGF were added to media on the day of use.

A.2 Hepatocyte culturing, cell evaluation methods and statistics

The cell suspension received from the Centrifuge and BRAT procedures were evaluated for viability and cell count using the Trypan Blue exclusion test in a Neubauer bright-line hemacytometer. The bowl volume employed in any BRAT procedure was randomly selected. To determine the effect of oxygenating the cells and media during the BRAT procedure, in three pairs of experiments flow cytometry was conducted on hepatocytes received after oxygenation had or had not occurred. After all procedures, media aliquots were tested for pathogens in order to determine the sterility of the procedures. In addition, after both centrifuge and BRAT procedures, aliquots containing 3.5-4 x 10⁶ cells were taken for seeding in 75 cm² cell culture flasks (Corning, Adcock Ingram, Johannesburg, SA) and subsequent culturing in a humidified CO₂ incubator at 37 degrees Celsius. Culture medium was changed 12 hours after seeding, and every 24 hours thereafter for 7 days. In order to determine the impact on hepatocyte cell cycle, flow cytometry of cells scraped from the cell culture flasks was performed 3 and 7 days after seeding.

Media samples were taken daily prior to changing the medium, to evaluate hepatocyte viability by means of LD and AST leakage and to examine the state of Cellular oxidation and Aerobic metabolism by means of the lactate to pyruvate ratio. Lactate and pyruvate concentrations were measured enzymatically, lactate at 520 nm and pyruvate at 340 nm on the Beckman Synchron LX system (Beckman kit 445875 and Sigma kit 726 respectively). The liver enzymes, lactate dehydrogenase (LD) and aspartate aminotransferase (AST) were also detected enzymatically at 340 nm using the Synchron LX system (Beckman Coulter kits 442655, 442665 respectively).

To allow the cells time to recover after the isolation procedure galactose elimination at Day 2 and urea production at Day 3 were investigated (results not presented in this study). On day 4 after isolation, cytochrome P450 activity was investigated by means of lidocaine clearance, by adding 500 µg/ml lidocaine and sampling once every hour for 3 hours. To measure lidocaine, an aliquot of the sample was spiked with bupivacaine as the internal standard. The proteins were precipitated with 1 M perchloric acid. After centrifugation, the supernatant was decanted and neutralized with 1M NaOH. Two extractions with dichloromethane followed and then the organic layers were combined and dried under a stream of dry nitrogen. The residue was redissolved in dichloromethane and analyzed by gas chromatography mass spectrometry. On completion of the lidocaine study, serum-free MEM replaced that in the flasks, and albumin production was investigated with sampling 24 hours later. Albumin concentration was determined colorimetrically by measuring at 600 nm on a Technikon RA-XT system (Miles Technikon method SM4-0131E94).

The Flow cytometry procedure involved the incubation of 1 ml of propidium iodide solution (Coulter DNA-Prep Reagents Kit) with 100 µL of a 2×10^6 cells/ml suspension, in the dark, for 30 minutes at room temperature. The samples were analyzed using a Beckman-Coulter Altra Flow Cytometer. A comparison of forward and side scatter data was used to gate the viable cells, in order to exclude debris from the population of cells present in the samples, while the DNA histograms indicated the relative cell cycle status of the suspension, that is, the proportion of DNA in the G0/G1, S or G2M phases. In order to examine if the cultured hepatocyte populations were proliferating normally and to determine if the isolation procedures had been sterile, daily examination of the culture flasks was performed using an Olympus CKX41 inverted microscope set for phase contrast. Digital micrographs, using an Olympus C4040 camera, were taken at day 3 and day 7 after the seeding of the culture flasks.

Statistical Analyses

GraphPad Prism 2.01 was used as a spreadsheet and Statistix 8 was used for the analysis of all data. Values are presented as the mean \pm the standard deviation. The lidocaine clearance and albumin production trends were calculated as follows: The raw data concentration values were converted to absolute quantities and graphed according to time. Straight lines were fitted to each set of results and the mean and standard deviation of the gradients of these lines were calculated. In the case of the lactate to pyruvate ratios and liver enzyme results, the mean and standard deviations were calculated according to each time interval in each experiment. Flow cytometry results were calculated as above,

and where appropriate, P values ($P < 0.05$) were calculated by the 2-tailed Mann-Whitney t-test for possible significant differences.

A.3 Cell culturing, metabolic evaluations and statistics

Daily sampling investigated lactate dehydrogenase (LD), aspartate aminotransferase (AST), glucose, lactate and pyruvate concentrations. These were measured using enzymatic kits. pO_2 , pCO_2 and pH were measured on a blood gas machine. The oxygen uptake rate (OUR) was calculated after sampling with the gas supply turned off.

Metabolic clearance/production studies were performed in both dynamic and static configurations as follows: on day 2 D(+)galactose elimination, using gas chromatography mass spectrometry (GC-MS) for detection; on day 3 ammonia detoxification (NH_4Cl) with urea synthesis, using enzymatic methods for detection. On day 4 lidocaine clearance, using LC-MS for detection; and on day 5 albumin production, using a spectrophotometric method. Upon termination on day 7, imaging studies involved either scanning electron microscopy (SEM), to investigate the presence of cells in the foam, or isotopic scanning to examine the seeded-distribution of active hepatocytes in the foam.

For SEM the method was as follows; Circulating medium was replaced with fixative: 2.5% glutaraldehyde in a 0.1 M phosphate buffer (PBS) at pH 7.4. After 30 minutes circulation the foam was removed and sections cut from the inlet, middle and outlet. After washing in PBS buffer these were placed in 1% Osmium tetroxide (OsO_4) for 30 minutes. Following water washes, the samples were dried in ethanol and mounted on aluminium plates. After high pressure CO_2 critical point drying for an hour the samples were gold sputtered and viewed with a JEOL JSM-840 Scanning Electron Microscope.

Radioactive labeling was performed by the active uptake of a 300 μCi dose of ^{99m}Tc -labeled-DISIDA N-(2,6-diisopropylacetanilide)-imino-diacetate which is metabolized only by active hepatocytes. This was injected into the medium and allowed to circulate for 6 minutes. The medium was drained and the circuit washed twice, after which the foam was removed and cut into three radial sections at the inlet, central and outlet portions along the bioreactor axis. These sections were placed on the inverted face of a low energy, high-resolution collimator of an Elscint Apex gamma camera, and scanned for 10 minutes.

Statistics: Microsoft Excel was used for data processing while Statistix 8 was used for analysis. Values are presented as the mean \pm standard deviation. Clearance/production rates were calculated by converting the raw data to absolute quantities and graphing according to time. The gradients of the linear fittings were taken to be the rates. Statistical significance was measured using Student's t test.



Table A.4.1 Modified-HGM cell culture media components

Component	Concentration
Deionized autoclaved H ₂ O	10 L/bottle of DMEM
*Powder DMEM +BSS,glutamine	equivalent for 10 L
NaHCO ₃	22 g for 10 L equivalent
*Streptomycin-Fungizone	10 ml/L
*Gentamycin sulphate	1 ml/L
*Fetal Calf Serum	100 ml/L
Insulin	mUnits/L
Glucagon	15-20 µg/L
Dexamethazone	67 µg/L
Epidermal Growth factor	20 µg/L
Transferrin (Fe ²⁺ saturated)	200 µl/L or 5-6 mg/L
DMSO	1 % v/v
Glucose	2 g/L
Galactose	2 g/L
Nicotinamide	0.610 g/L
Zinc chloride	0.544 mg/L
Zinc sulphate	0.750 mg/L
Cupric sulphate	0.2 mg/L
Manganese sulphate	0.025 mg/L
Sodium selenite	5-6 µg/L

Note: All items except * purchased from Sigma-Aldrich, Johannesburg, South Africa.
*’s were purchased from Bio-Whittaker, Adcock Ingram Scientific, Johannesburg, South Africa

Appendix B: *In vivo* study methods

B.1 Anesthesia protocol

Carprofen (Rimadyl[®], 5 mg/kg BW SC) was injected pre-operatively, followed by isoflurane (Safe Line pharmaceuticals) inhalation using a Boyle's iso-for inhalation machine with 100 % O₂. Buprenorphine (Temgesic[®], 0.1 ml/100g BW IM) was given at the time of incision. To manage pain post-operatively, carprofen was given once daily with buprenorphine adjusted to 30 % of normal liver weight every 12 hrs. On termination, all animals were euthanased through inhalation of a lethal overdose of isoflurane.

Recovery, pain and toxicity scoring

The National Society for the Protection and Care of Animals (NSPCA) pain and toxicity scoring sheets were completed once daily to assess possible toxicity, pain and humane end-points for the experiments.

Statistics

Microsoft Excel (ver. 2003) was used as a spreadsheet while Statistix (ver. 8, Tallahassee, FL, USA) was used for data analysis. The mean and standard deviations were calculated for all variables. Non-parametric Wilcoxon rank sum tests, appropriate for small groups, were used to determine the statistical significance of differences between groups.

B.2 Animal preparation

Pathogen-free pigs were purchased from a herd two weeks prior to each experiment to allow for quarantine and acclimatisation. They were housed in environmentally controlled stables (25°C) with a 12 hr light/dark cycle (University of Pretoria Biomedical Research Centre). Food was composed of a standard pig diet (EPOL) and water until fasting commenced 24 hours prior to each experiment. Energy and electrolytes (Rehidrat, Pfizer) were supplemented during the daytime (08:00-16:00). At 16:00 lorazepam was administered (2 mg IM, Ativan, Aspen) by using a pole-syringe (Dan-Inject) followed by an antibiotic (1g IV, Ceftriaxone, Pharmacare) as intestinal flora prophylaxis. Each pig was hence kept nil per mouth until commencement at 07.00 the following morning.

Anaesthesia protocol

The pigs were immobilized by IM injection of midazolam (0.3 mg/kg, Dormicum, Roche) and ketamine (10 mg/kg, Anaket, Centaur). A 20G IV Teflon catheter (Jelco, Johnson & Johnson) was placed in the ear vein for induction of anesthesia with propofol (3 mg/kg, Diprivan, Astra Zeneca) and intubation with a 7.5 mm endotracheal tube. A nasogastric tube was placed per os to deflate the stomach. After sterile preparation the animal was transferred to the theatre where it was immobilized in the supine position and draped for abdominal surgery. Anaesthesia was maintained with 1.5% isoflurane in an air-oxygen mixture with the aid of a circle rebreathing anaesthetic machine with carbon dioxide absorption (Procure 500, Ohmed, Scientific Group). Fresh gas flow rate was set

at 300 ml/min for oxygen and 600 ml/min for air. Minute volume was maintained with positive pressure ventilation (Ohmeda 7000 Ventilator) to maintain end-tidal carbon dioxide partial pressure in the range of 35-40 mmHg. Intra and postoperative analgesia was supplemented with the lumbar epidural administration of ropivacaine (0.2 ml/kg, Naropin, Astra) and morphine sulphate (0.1 mg/kg, morphine sulphate-Fresenius amps, Fresenius Kabi). Ceftriaxone (1g, Pharmicare) was administered IV as before. Blood volume and blood glucose were maintained with 5% dextrose in a balanced electrolyte solution (Intramed, Ringer Lactate) administered at 10 ml/kg/hr for the duration of anesthesia. All pulse-oximetry (TL-101T, Nihon Kohden, Medical Systems), CO₂ (TG-900P, Nihon Kohden, Medical Systems), electrocardiographic (ECG) (BR-903P, Nihon Kohden, Medical Systems) and electroencephalographic (EEG) electrodes were attached to the animal at this time. Prior to liver devascularization, 500 ml of a gelatin plasma-expander (20 ml/kg IV, gelofusine, B/Braun) was administered IV. This dose was repeated immediately following liver devascularization. Perioperatively, arterial blood pressure was maintained at a mean pressure of between 60-80mmHg (MX 950 Transtar Pressure Transducers, Medex Medical) with the IV infusion of phenylephrine (2-25 µg/kg/min phenylephrine, Covan). Core body temperature was maintained as near as possible to 37.5 degrees C using forced hot air (Bair hugger 505, Augustine Medical).

Catheter placement

Prior to the liver devascularization procedure, an arterial catheter (G16, 115.17 Vigon, Viking Medical) was placed in the common carotid artery for monitoring arterial pressures and blood gases. The external jugular vein was exposed for cannulation with a vascath (CS 15123E, Arrow) and a double lumen venous catheter (CV50688 Fr 7, Arrow) was inserted into the lumen of the internal jugular vein for monitoring central venous pressure (CVP). Positioning was verified after connection of the respective catheters to the monitors. A supra-pubic cystostomy was also performed prior to closing the abdomen using a 10 fg Foleys catheter to monitor urine output

Intensive care

Following surgery the animal was transferred to an intensive care unit (ICU). Continuous ventilation was maintained (40% O₂, tidal volume 10-15 ml/kg) with a post expiratory pressure (PEEP) of 5 mmHg (Ventilator 7200a, Puritan-Bennet). Settings were adjusted hourly according to arterial blood gas (ABG). Sedation was maintained by infusing midazolam (0.3 mg/kg/hr Dormicum, Roche), fentanyl (0.02 mg/kg/hr Fentanyl, Janssen) and pentobarbitone (4 mg/kg/hr Pentobarbitone, 6%, Kyron) with infusion pumps (Modular 3000, Smith's Medical). Boluses of muscular relaxant (0.3 mg/kg/hr Esmeron, Sanofi Synthelabo) were administered IV when necessary. Hemodynamic stability was regulated according to CVP (no less than 14 mmHg) and urine output (2 ml/kg/hr) using fluid boluses including Ringer's lactate (Adcock Ingram) and colloid (Gelofusine, B/Braun). Blood glucose was maintained using 50% glucose (Adcock Ingram) to prevent hypoglycaemia. Dobutamine (2.5-10 µg/kg/min Dobutrex, Eli Lilly) and Phenylephrine (1 µg/kg/min Phenylephrine, Knoll) were titrated to maintain mean arterial blood pressure at a minimum of 60mmHg. Blood potassium (3.4-4.5 mmol/l) and sodium (135-145 mmol/l) concentrations were maintained using Potassium chloride (Adcock Ingram) and Sodium chloride (Adcock Ingram). Heparin was titrated according to activated

clotting time (ACT). Bolus doses (3-5 units/kg) was administered IV until the ACT (as measured by a Hemochron JR, Brittan Health Care) returned to normal (220-250 secs). Body temperature was maintained as above. Intensive care was maintained until the cessation of cardiac function, which was defined as the point of death in this study.

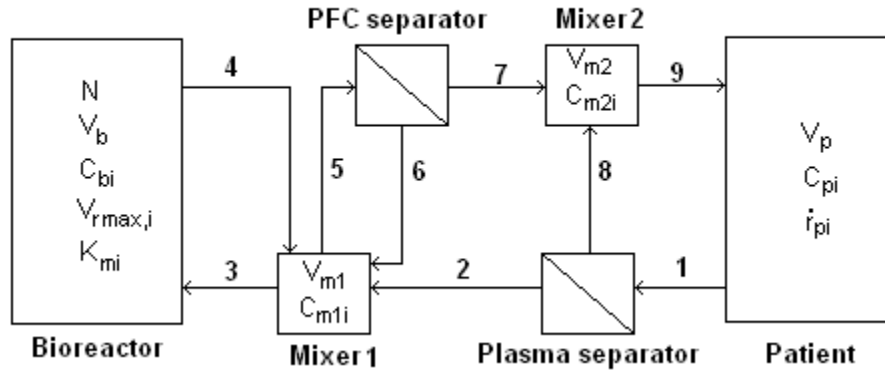
Clinical measurements

Systemic and biochemical indices were measured for the duration of each experiment (table 4.1). Arterial blood pressure and Central venous pressure (CVP) were connected to a calibrated electronic pressure transducer (MX9522, Medex, SSEM). A multiparameter patient monitor (BMM-10-1K, Gambro and BSM 4103K Nihon Kohden) was used to monitor the ECG, pulse rate, CVP, systolic-, diastolic-, mean arterial blood pressure and haemoglobin saturation with the aid of a pulse oximeter probe placed on the tongue. End-tidal CO₂ partial pressure was measured with an in-line sensor placed between the endotracheal tube connection and the breathing circuit. Rectal temperature and ABG measurements were performed hourly while blood biochemical samples were taken four-hourly. Standard [human] laboratory methods were used for these indices. Continuous EEG measurement was performed until termination. A diagrammatic drawing of the brain structure was superimposed on the external bone features and a standardized measuring protocol was adapted from the International 10/20 electrode placement system for humans. Subcutaneous needle electrodes were used for registering activities at the frontal, central, temporal and occipital regions of the brain. A digital recording system was used for EEG monitoring (Medtronic Walter Graphtek PL-EEG, Medtronic) and a software package (Neuro, Galileo NT version 2.31/00, Medtronic) was used for digital spectral Fast Fourier Transform (FFT) analysis. Frequency spectra of 10-second epochs were used in the analysis. In this study we describe only the alpha (8-15 Hz), total delta (0-4 Hz) and relative power values in the frontal and central regions of the brain. All clinical measurements were terminated at death.

Appendix C: The derivation of the compartmental model equations

C.1 System model diagram

The figure below is a simplified representation of the BALSS system connected to a patient, with basic notation and stream (flow-circuit) numbers.



C.2 Model Notation

Symbol	Description	Units
C_{ai}	Concentration of component i in stream a	$\text{mol } i / \text{m}^3$
C_{xi}	Concentration of component i in compartment x	$\text{mol } i / \text{m}^3$
f_i	Fraction of substrate i that is unbound	
g	Ratio of filtrate to feed flow rates for PFC separator	
H_a	Hematocrit in stream $a = (\text{Volume cellular components}) / (\text{Volume plasma} + \text{Volume cellular components})$	
$K_{m,i}$	Michaelis constant for substrate i	$\text{mol } i / \text{m}^3$
n_{xi}	Number of moles of component i in compartment x	$\text{mol } i$
\dot{n}_{ai}	Molar flow rate of component i in stream a	$\text{mol } i / \text{s}$
N	Number of hepatocytes in bioreactor	cells
Q_a	Volumetric plasma flow rate of stream a (i.e. excluding PFC and cellular blood components)	m^3 / s
$Q_{a,pfc}$	Volumetric flow rate of stream a , including PFC = $Q_a / (1 - \phi_a)$	m^3 / s
$Q_{a,ct}$	Volumetric flow rate of stream a , including cellular blood components = $Q_a / (1 - H_{ct,a})$	m^3 / s
r_{xi}	Reaction rate of component i in compartment x	$\text{mol } i / \text{m}^3 \cdot \text{s}$
t	Time	s
$V_{\max,i}$	Maximal rate of metabolism for substrate i	$\text{mol } i / \text{m}^3 \cdot \text{s}$
V_x	Volume of compartment x , excluding PFC and cellular blood component volume	m^3
$V_{x,pfc}$	Volume of compartment x , including PFC = $V_x / (1 - \phi_x)$	m^3
$V_{x,ct}$	Volume of compartment x , including cellular blood components = $V_x / (1 - H_x)$	m^3

Greek symbols

ϕ_a Volume fraction of PFC (perfluorocarbon) in stream a

General subscripts

0 Value of variable at time zero
 a Stream a
 b Bioreactor
 ct Includes cellular blood components
 $m1$ Mixer 1
 $m2$ Mixer 2
 p Patient
 pl Plasma
 t Constituent / toxin i
 x Compartment x

C.3 Input parameters (with typical/indicative values for the UP-CSIR BALSS, where available)

Parameter	Description	Typical value	Units
$C_{bi,0}$	Starting concentration of component i in bioreactor		0 mol/m^3
$C_{m1i,0}$	Starting concentration of component i in mixer $m1$		0 mol/m^3
$C_{m2i,0}$	Starting concentration of component i in mixer $m2$		0 mol/m^3
$C_{pi,0}$	Starting concentration of component i in patient	0.07	mol/m^3
f_i	Fraction of total substrate i that is unbound	1	
g	Filtrate to feed flow rate for PFC separator	0.025	
H_8	Hematocrit of plasma separator concentrate	0.8	
H_p	Hematocrit in patient	0.5	
K_{mi}	Michaelis constant for substrate i	20.86	$\text{mol } i / \text{m}^3$
N	Number of hepatocytes in bioreactor	1×10^{10}	cells
$Q_{1,ct}$	Rate of withdrawal of blood from patient	2×10^{-6}	m^3/s
$Q_{3,pfc}$	Flow rate of plasma-PFC blend into bioreactor	8.33×10^{-6}	m^3/s
r_{pi}	Rate of reaction of component i in patient	3.56×10^{-8}	$\text{mol/m}^3 \cdot \text{s}$
$V_{b,pfc}$	Volume of bioreactor	0.0003	m^3
V_{rmax}	Maximum metabolic rate of hepatocytes	3.1×10^{-11}	$\text{mol/s} \cdot \text{cell}$
$V_{m1,pfc}$	Volume of mixer $m1$	0.00065	m^3
$V_{m2,ct}$	Volume of mixer $m2$	0.0001	m^3
$V_{p,ct}$	Volume of blood in patient	0.004	m^3
ϕ_3	Volume fraction PFC in stream 3	0.1	

C.4 Output parameters

$$C_{pi}, C_{bi}, C_{m1i}, C_{m2i}$$

C.5 Variables that influence the outputs,

g

f_i

N

$$V_p, V_b, V_{m1}, V_{m2}$$

$$C_{pi,0}$$

$$V_{\max,i}, K_{mi}, r_{pi}$$

$$Q_{1,ct}, Q_3$$

C.6 Basic assumptions

1. Constituent i is well mixed in the bioreactor (b), patient (p), mixer 1 ($m1$) and mixer 2 ($m2$) (i.e. these vessels are modeled as continuously stirred tank reactors).
2. Both plasma and PFC separators have 100% separation efficiency (i.e. no cellular blood components pass into stream 2, and no PFC (perfluorocarbon) emulsion droplets pass into stream 7).
3. Volumes of lines and separators are negligible.
4. Separators do not differentially separate plasma constituents (i.e. filtrate and concentrate have the same plasma constituent concentrations).
5. Changes in stream volumetric flow rates due to reactions are negligible.
6. PFC does not absorb any plasma components/constituents in significant quantities.
7. Rate of production in patient ($r_{pi}V_p$) is the net rate (i.e. production by body – clearance by body – excretion by body).
8. Bioreactor clearance rates are determined by cell number and by toxin concentration.
9. Mixer 2 is a combination of the two physical reservoirs (the plasma and blood reservoirs).

C.7 Flow rates

The total blood flow rate of stream 1, $Q_{1,ct}$, is an input parameter. The flow rate of stream 8, $Q_{8,ct}$, can be calculated from the known hematocrit (H) levels in streams 1 and 8, where the definition of hematocrit in this document is defined as the volume fraction of cellular components in the total blood stream:

$$Q_{8,ct} = \frac{H_1}{H_8} Q_{1,ct} \tag{C.1}$$

$$Q_8 = \frac{(1-H_8)}{(1-H_1)} \frac{H_1}{H_8} Q_1$$

where $H_I = H_p$

The flow rate of stream 2:

$$Q_2 = Q_1 - Q_8 \quad (C.2)$$

The return flow rate of blood to the patient must be equal to the flow rate of blood extracted from the patient:

$$Q_9 = Q_1 \quad (C.3)$$

The flow rate of stream 7 can now be calculated:

$$Q_7 = Q_9 - Q_8 \quad (C.4)$$

The exit flow rate from the bioreactor must be equal to the inlet flow rate:

$$Q_4 = Q_3 \quad (C.5)$$

The ratio of filtrate flow rate to inlet flow rate for the PFC separator, g , is given by:

$$g = Q_7 / Q_5 \quad (C.6)$$

$$\therefore Q_5 = Q_7 / g$$

The concentrate flow rate from the PFC separator is now given by:

$$Q_6 = Q_5 - Q_7 \quad (C.7)$$

$$Q_6 = Q_7(1/g - 1)$$

C.8 Concentrations

The number of moles of component i in compartment x is given by:

$$n_{xi} = C_{xi} V_x \quad (C.8)$$

The molar flow rate of component i in stream a is given by:

$$\dot{n}_{ai} = C_{ai} Q_a \quad (C.9)$$

Because of the assumption of good mixing, the concentration of a constituent in the exit streams from any vessel is equal to the concentration of the same constituent in the vessel at any given time:

$$C_{1i} = C_{pi}$$

$$C_{9i} = C_{m2i} \quad (C.10)$$

$$C_{3i} = C_{5i} = C_{m1i}$$

$$C_{4i} = C_{bi}$$

Because no concentration changes occur in the separators, separator exit concentrations are equal to separator inlet concentrations:

$$C_{2i} = C_{8i} = C_{1i} \quad (C.11)$$

$$C_{6i} = C_{7i} = C_{5i}$$

C.9 Molar balances

Taking a mole balance for component i over the patient:

$$\begin{aligned} \frac{dn_{pi}}{dt} &= \text{production} - \text{consumption} + \text{in} - \text{out} \\ \frac{d(V_p C_{pi})}{dt} &= r_{pi} V_p - 0 + C_{9i} Q_9 - C_{1i} Q_1 \end{aligned} \quad (\text{C.12})$$

Substituting from equation (C.10), and rearranging:

$$\begin{aligned} V_p \frac{dC_{pi}}{dt} &= r_{pi} V_p + C_{m2i} Q_9 - C_{pi} Q_1 \\ \frac{dC_{pi}}{dt} &= r_{pi} + \frac{Q_9}{V_p} C_{m2i} - \frac{Q_1}{V_p} C_{pi} \end{aligned} \quad (\text{C.13})$$

Similarly, taking a mole balance over the bioreactor:

$$\begin{aligned} \frac{dn_{bi}}{dt} &= \text{production} - \text{consumption} + \text{in} - \text{out} \\ \frac{d(V_b C_{bi})}{dt} &= 0 + r_{bi} V_b + C_{3i} Q_3 - C_{4i} Q_4 \end{aligned} \quad (\text{C.14})$$

Substituting from equation (C.10) and rearranging:

$$\begin{aligned} V_b \frac{dC_{bi}}{dt} &= r_{bi} V_b + C_{mli} Q_3 - C_{bi} Q_4 \\ \frac{dC_{bi}}{dt} &= \frac{Q_3}{V_b} C_{mli} - \frac{Q_4}{V_b} C_{bi} + r_{bi} \end{aligned} \quad (\text{C.15})$$

Taking a mole balance over mixer $m1$:

$$\begin{aligned} \frac{dn_{m1i}}{dt} &= \text{production} - \text{consumption} + \text{in} - \text{out} \\ \frac{d(V_{m1} C_{m1i})}{dt} &= 0 - 0 + C_{2i} Q_2 + C_{6i} Q_6 + C_{4i} Q_4 - C_{3i} Q_3 - C_{5i} Q_5 \end{aligned} \quad (\text{C.16})$$

Substituting from equations (C.10) and (C.11), and rearranging:

$$\begin{aligned} V_{m1} \frac{dC_{m1i}}{dt} &= C_{pi} Q_2 + C_{mli} Q_6 + C_{bi} Q_4 - C_{mli} Q_3 - C_{mli} Q_5 \\ \frac{dC_{m1i}}{dt} &= \frac{Q_2}{V_{m1}} C_{pi} + \frac{Q_4}{V_{m1}} C_{bi} + \frac{(Q_6 - Q_3 - Q_5)}{V_{m1}} C_{mli} \end{aligned} \quad (\text{C.17})$$

Taking a mole balance over mixer $m2$:

$$\begin{aligned}\frac{dn_{m2i}}{dt} &= \text{production} - \text{consumption} + \text{in} - \text{out} \\ \frac{d(V_{m2}C_{m2i})}{dt} &= 0 - 0 + C_{8i}Q_8 + C_{7i}Q_7 - C_{9i}Q_9\end{aligned}\quad (\text{C.18})$$

Substituting from Equations (C10) and (C11), and rearranging:

$$\begin{aligned}V_{m2} \frac{dC_{m2i}}{dt} &= C_{pi}Q_8 + C_{mli}Q_7 - C_{m2i}Q_9 \\ \frac{dC_{m2i}}{dt} &= \frac{Q_8}{V_{m2}}C_{pi} + \frac{Q_7}{V_{m2}}C_{mli} - \frac{Q_9}{V_{m2}}C_{m2i}\end{aligned}\quad (\text{C.19})$$

C.10 Rates of production/clearance

The production rate (r_{pi}) of component i in the patient is assumed to be constant. The rate of clearance/metabolism of component i in the bioreactor can be approximated using the Michaelis-Menten relationship [91]:

$$\text{Rate of metabolism} = r_{bi} = \frac{V_{\max,i}C_{bi}f_i}{K_{mi} + C_{bi}f_i}\quad (\text{C.20})$$

When $C_{mli}f_i \gg K_{mi}$, then the rate of metabolism = $V_{\max,i}$. When $C_{mli}f_i \ll K_{mi}$, then the rate of metabolism = $V_{\max,i}f_i C_{mli}/K_{mi}$. The Michaelis-Menten parameters ($V_{\max,i}$ and K_{mi}) can be determined from a single compartment bolus experiment by rewriting Equation (A.20), as follows:

$$\begin{aligned}\frac{dC_i}{dt} = r_i &= -\frac{V_{\max,i}C_i f_i}{K_{mi} + C_i f_i} \\ -\frac{dt}{dC_i} &= -\frac{1}{r_i} = \frac{K_{mi}}{V_{\max,i}C_i f_i} + \frac{1}{V_{\max,i}}\end{aligned}\quad (\text{C.21})$$

Thus a plot (called a Lineweaver-Burk plot) of $1/r_i$ vs. $1/C_i$ should yield a straight line with y-intercept $1/V_{\max,i}$ and gradient $K_{mi}/V_{\max,i}f_i$.

The V_{\max} value determined from the plot is dependent on enzyme concentration (e.g. if enzyme concentration doubles, V_{\max} doubles), while K_m is not [91]. If one assumes that enzyme concentration is directly proportional to hepatocyte ‘concentration’ (i.e. hepatocytes per reactor volume), then one can calculate a reduced maximum reaction rate ($V_{r\max}$, with units mol/s.cell) from the experimentally determined V_{\max} value as follows:

$$\begin{aligned}V_{r\max} &= \frac{V_{\max}V_b}{N} \\ \text{and } V_{\max} &= \frac{V_{r\max}N}{V_b}\end{aligned}\quad (\text{C.22})$$

This reduced maximum reaction rate can now be used to estimate V_{\max} for different reactor sizes and hepatocyte loadings.

Using equation (C.20), equation (C.15), can now be rewritten as:

$$\begin{aligned}
 V_b \frac{dC_{bi}}{dt} &= r_{bi} V_b + C_{mli} Q_3 - C_{bi} Q_4 \\
 V_b \frac{dC_{bi}}{dt} &= -\frac{V_{\max,i} C_{bi} f_i V_b}{K_{mi} + C_{bi} f_i} + C_{mli} Q_3 - C_{bi} Q_4 \\
 \frac{dC_{bi}}{dt} &= -\frac{V_{\max,i} C_{bi} f_i}{K_{mi} + C_{bi} f_i} + \frac{Q_3}{V_b} C_{mli} - \frac{Q_4}{V_b} C_{bi}
 \end{aligned} \tag{C.23}$$

C.11 Summary of equations and parameters

$$\begin{aligned}
 \frac{dC_{pi}}{dt} &= r_{pi} + \frac{Q_9}{V_p} C_{m2i} - \frac{Q_1}{V_p} C_{pi} \\
 \frac{dC_{bi}}{dt} &= -\frac{V_{\max,i} C_{bi} f_i}{K_{mi} + C_{bi} f_i} + \frac{Q_3}{V_b} C_{mli} - \frac{Q_4}{V_b} C_{bi} \\
 \frac{dC_{mli}}{dt} &= \frac{Q_2}{V_{m1}} C_{pi} + \frac{Q_4}{V_{m1}} C_{bi} + \frac{(Q_6 - Q_3 - Q_5)}{V_{m1}} C_{mli} \\
 \frac{dC_{m2i}}{dt} &= \frac{Q_8}{V_{m2}} C_{pi} + \frac{Q_7}{V_{m2}} C_{mli} - \frac{Q_9}{V_{m2}} C_{m2i}
 \end{aligned} \tag{C.24}$$

These equations are supported by the following set of algebraic equations:

$$\begin{aligned}
 Q_8 &= \frac{(1-H_8)}{(1-H_1)} \frac{H_1}{H_8} Q_1 \\
 Q_2 &= Q_1 - Q_8 \\
 Q_9 &= Q_1 \\
 Q_7 &= Q_9 - Q_8 \\
 Q_4 &= Q_3 \\
 Q_5 &= Q_7/g \\
 Q_6 &= Q_7(1/g - 1) \\
 C_{1i} &= C_{pi} \\
 C_{9i} &= C_{m2i} \\
 C_{3i} &= C_{5i} = C_{mli} \\
 C_{4i} &= C_{bi} \\
 C_{2i} &= C_{8i} = C_{1i} = C_{pi} \\
 C_{6i} &= C_{7i} = C_{5i} = C_{mli}
 \end{aligned} \tag{C.25}$$



Calculation of flow rates and volumes from input parameters:

$$\begin{aligned}Q_1 &= Q_{1,ct} (1 - H_p) \\Q_3 &= Q_{3,pfc} (1 - \phi_3) \\V_p &= V_{p,ct} (1 - H_p) \\V_b &= V_{b,pfc} (1 - \phi_3) \\V_{m1} &= V_{m1,pfc} (1 - \phi_3) \\V_{m2} &= V_{m2,ct} (1 - H_{ct,p})\end{aligned}\tag{C.26}$$

Calculation of PFC volume fraction in stream 6:

$$\begin{aligned}\phi_5 Q_5 &= \phi_6 Q_6 + \phi_7 Q_7 \\ \text{But } \phi_7 &= 0 \\ \therefore \phi_5 Q_5 &= \phi_6 Q_6 \\ \phi_6 &= \frac{Q_5}{Q_6} \phi_5\end{aligned}\tag{C.27}$$

Appendix D: *On line* model sensitivity and verification

Table D.1 Numerical associations in and between classes

Association	Variable 1	Variable 2	Pearson correlation > 0.4	Spearman correlation > 0.3	Comments
Internal	ave_pH	rLactate	-0.71	-0.47	sources of change in pH
	ave_pH	ave_pCO ₂	-0.67	-0.47	
	ave_pH	ave_HCO ₃	+0.46	+0.58	
	ave_Pulse	rNa ⁺	-0.61	-0.33	electrolyte effect
	rK ⁺	rCreatinine	+0.87	+0.64	kidney indices related
	rCreatinine	Urine_Tot	-0.72	-0.70	
	rBilirubin	rALP	+0.46	+0.59	Liver indices related
	rBilirubin	rALT	+0.73	+0.78	
	rBilirubin	rAST	+0.66	+0.74	
	rBilirubin	rLD	+0.48	+0.73	
	rAmmonia	rBcAA/AroAA	+0.79	-0.39	
	rAmmonia	rAST	+0.53	+0.56	
	rAmmonia	rLD	+0.74	+0.37	
	Fr_a/d_fr	Pw_a/d_fr	-0.47	-0.57	
	rPT	rAPTT	-0.49	-0.30	Coagulation indices
	rPT	rAntiThrombin	+0.79	+0.68	
	rPT	rFibrinogen	+0.46	+0.31	
	rFibrinogen	rAntiThrombin	+0.81	+0.61	
	rFactor II	rFactor VII	+0.71	+0.66	
	rFactor VII	rFactor X	+0.69	+0.52	
rFactor II	rFactor X	+0.44	+0.40		
rAmmonia	Fr_a/d_fr	-0.79	-0.54	Encephalopathy and the liver	
rAmmonia	Fr_a/d_ct	-0.42	-0.36		
rAmmonia	Pw_a/d_fr	+0.38	+0.43	Encephalopathy and *Fischer's ratio	
rBcAA/AroAA	Fr_a/d_fr	+0.90	+0.75		
rBcAA/AroAA	Fr_a/d_ct	+0.61	+0.43		
rBcAA/AroAA	Pw_a/d_fr	-0.47	-0.43		
rGlutamine	Fr_a/d_fr	-0.61	-0.46	Encephalopathy and glutamine	
rGlutamine	Fr_a/d_ct	-0.40	-0.57		
rGlutamine	Pw_a/d_fr	0.92	+0.93	Encephalopathy and lactate	
rLactate	Fr_a/d_fr	-0.96	-0.64		
rLactate	Fr_a/d_ct	-0.86	-0.89		
rLactate	Pw_a/d_fr	+0.47	+0.64		
rPyr	Fr_a/d_ct	-0.57	-0.39		
rPyr	Pw_a/d_fr	+0.48	+0.64		
rCreatinine	rGlutamine	+0.61	+0.43		Kidney function and *AAs
rCreatinine	rPT	+0.43	+0.72		Coagulopathy and the kidneys
rCreatinine	rFibrinogen	-0.44	-0.39		
rCreatinine	rAmmonia	+0.78	+0.35	Liver and kidneys	
Urine_Tot	rHkt	+0.59	+0.53	The effect of fluids on hematocrit	
Fluids_Tot	rHkt	+0.52	+0.46		
rHb	rHkt	+0.81	+0.68		

Notes: 1. Inclusion in the table required a Pearson coefficient > 0.4 and a Spearman coefficient > 0.3.

2. prefixes: r = rate of change over time, and ave_ = average over time. 3. All variables with Fr_a/d were for indices of electro-encephalograms (EEG), which were measured in the animal experiments, but have shown no prognostic value. BcAA/AroAA = Fischer's ratio, where AAs = amino acids (see section 4.2).

D.2 First-order assumptions

The assumption of the linearity over time of the composing first order equations was investigated by determining the best-fit linear equation for each data for all variables. A mean R^2 value, the numerical square of the Pearson coefficient (and the proportion of the variance in the dependent variable attributable to the variance in each independent variable) was calculated for all variables (figure D.2.1). The majority of the variables had R^2 values above 0.5 (Pearson coefficients > 0.7) which indicated that they mostly linear and justified the numerical design of the model. Of interest was a strong correlation between the variables that exhibited the greatest change, that is, the highest P values (table 4.2.2) and those that were most linear over time. Variables that had R^2 values < 0.5 , but which were still felt to possess some prognostic value were weighted to relatively decrease their contribution to the eventual prediction. Specifically, a percentile weight was used related to their linearity. In general, the variables used for prediction during the surgical interval ($T < 0$) had lower R^2 values (were less linear) than those used during the ICU period ($T > 0$). This validated the use of a larger number of variables in the $T < 0$ period, each with relatively less weight than in the $T > 0$ period. It was also expected that the $T < 0$ part would be less accurate than the $T > 0$ part.

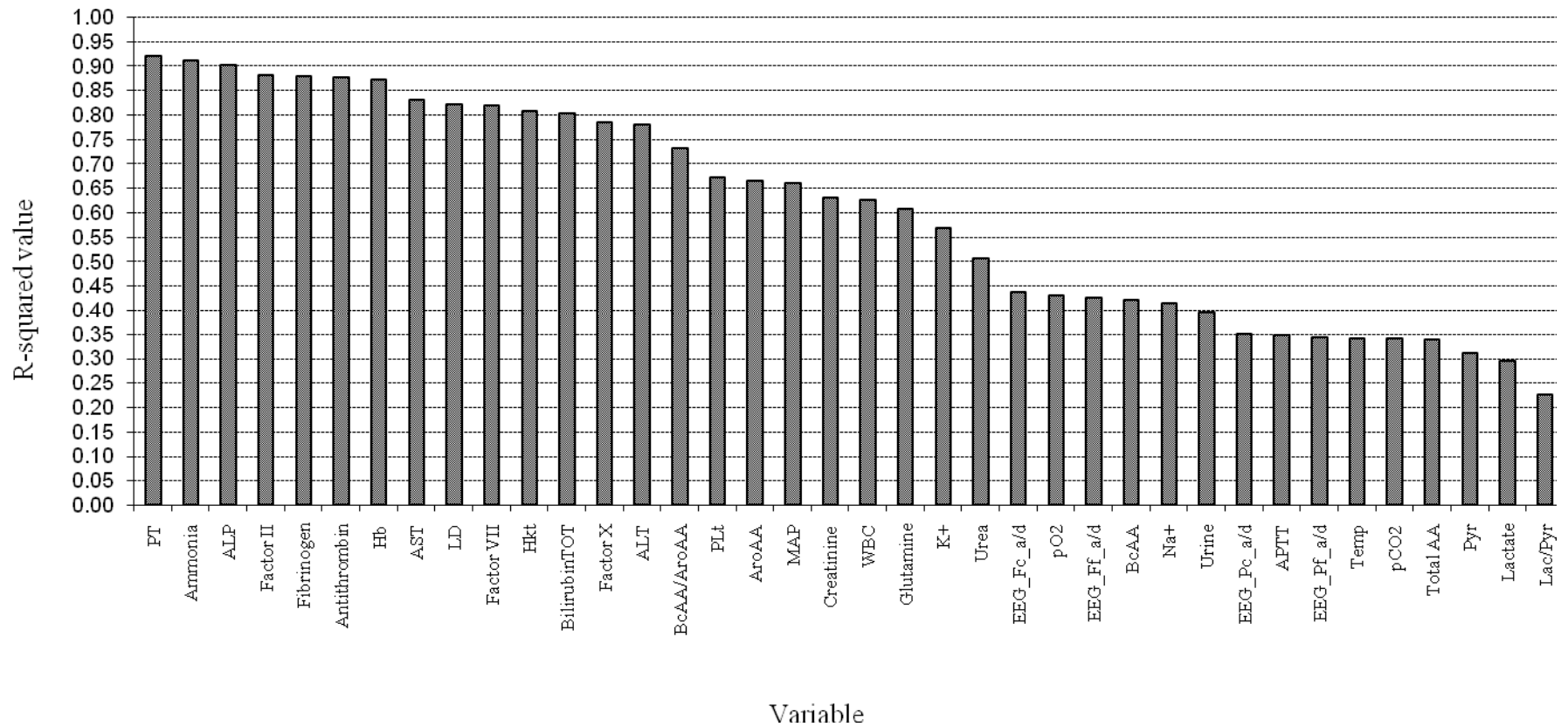


Figure D.2.1 Linearity of variable trends. The majority of measured variables demonstrated an R^2 value above magnitude 0.5.

D.3 Model sensitivity

1. Tornado diagrams [285] function as a macro in Excel and require the specification of a high and low value for each of the input variables of the model. The output is then displayed in terms of each of the composing variables' ranges about the mean predicted value. Thus, the dependence of the model's output on each of the inputs is visible. i.e. the larger the particular input variable's range about the summated mean predicted value, as determined by the weight appropriated to that variable, the greater the influence that variable has on the model's output. The data range used for the diagrams below was that measured in practice (section 5.2). The method assumes the Gaussian normality of the input populations. Only a selection of the BI Tornado diagrams are presented below:

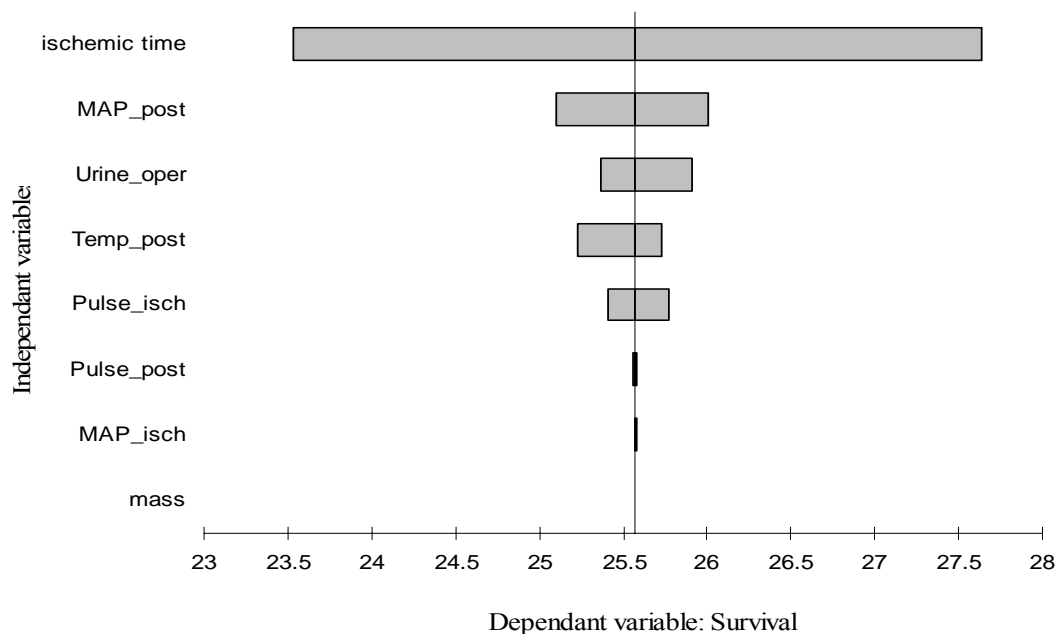


Figure D.3.1 Tornado diagram for PI model (T<0)

Note: The Ischemic time clearly has the greatest impact on Survival during the surgical interval. Output sensitivity is determined by the weight appropriated to each variable.

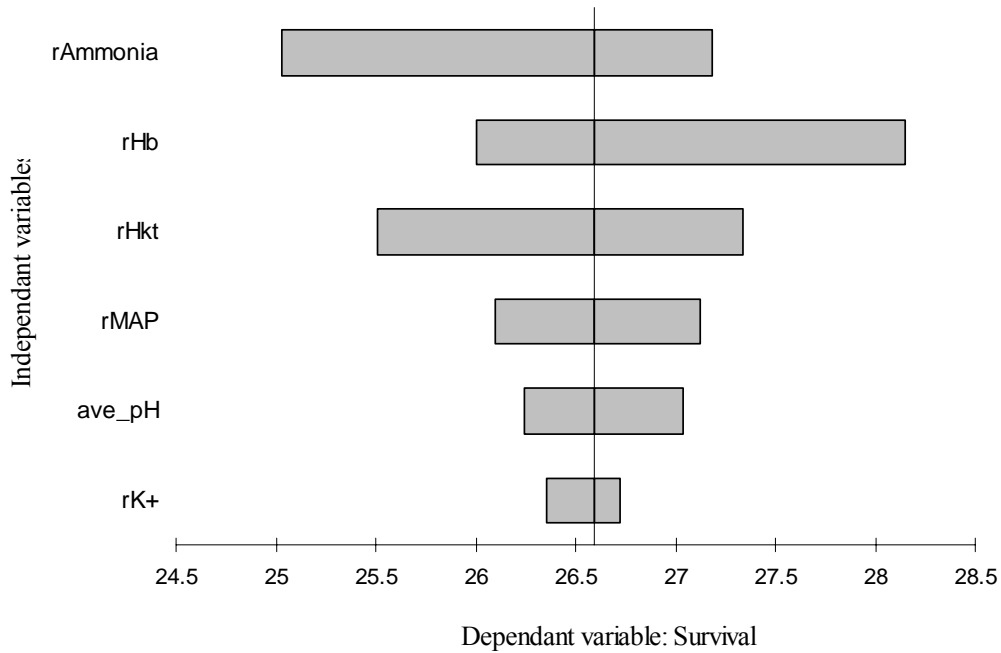


Figure D.3.2 Tornado diagram for PI model ($T > 0$)

Note: The rate of increase of blood Ammonia most strongly impacted Survival after surgery. Output sensitivity is determined by the weight appropriated to each variable.

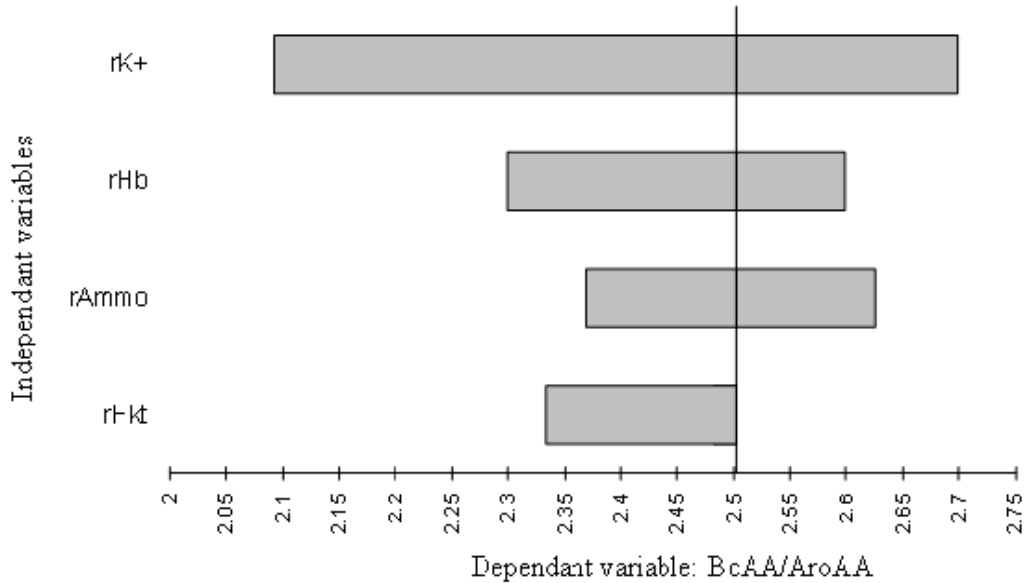


Figure D.3.3 BI Model Sensitivity for BcAA/AroAA (BI) (at 12 hrs)

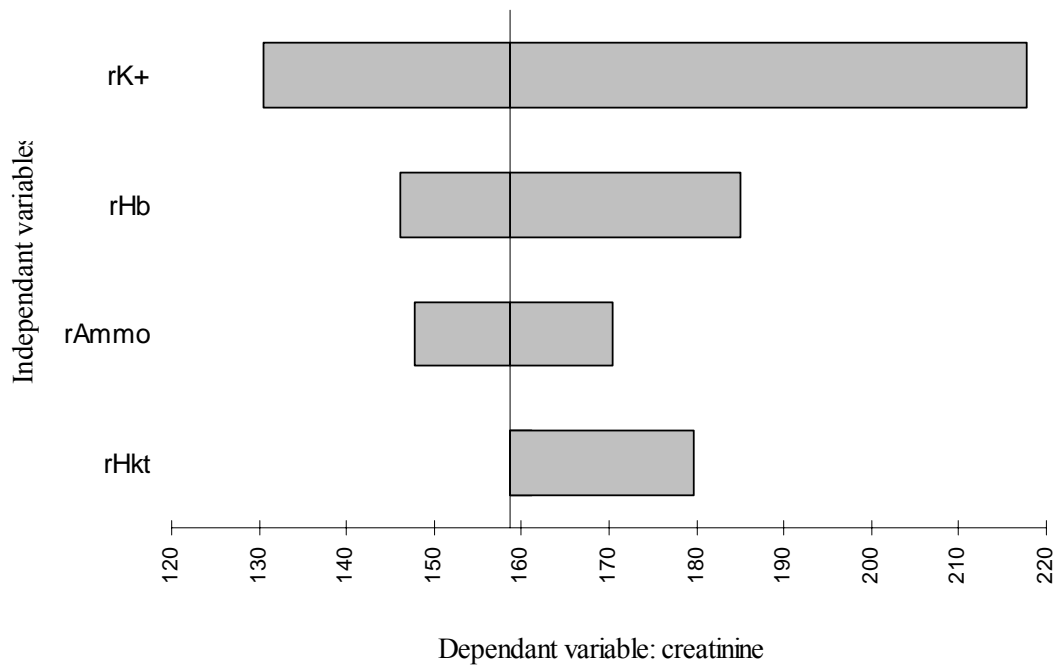


Figure D.3.4 BI Model sensitivity for creatinine (at 12 hrs)

2. Monte Carlo simulation

This procedure [285-287] was used to determine the sensitivity of the model's outputs to generated random numbers as inputs. The model was programmed into an Excel spreadsheet then 1000 random numbers, parameterized about the measured mean and standard deviation for each variable, were generated. This data was used as input to the model. Output sensitivity was determined individually and in combination. i.e. either one variable was randomized independently while retaining all other variables on their mean values, or all variables were randomized simultaneously, followed by the summation of the results. This method of analysis assumes normality in the input data. The latter assumption was also tested by using the same procedure but with uniformly distributed populations of generated numbers. The results were then graphically projected:

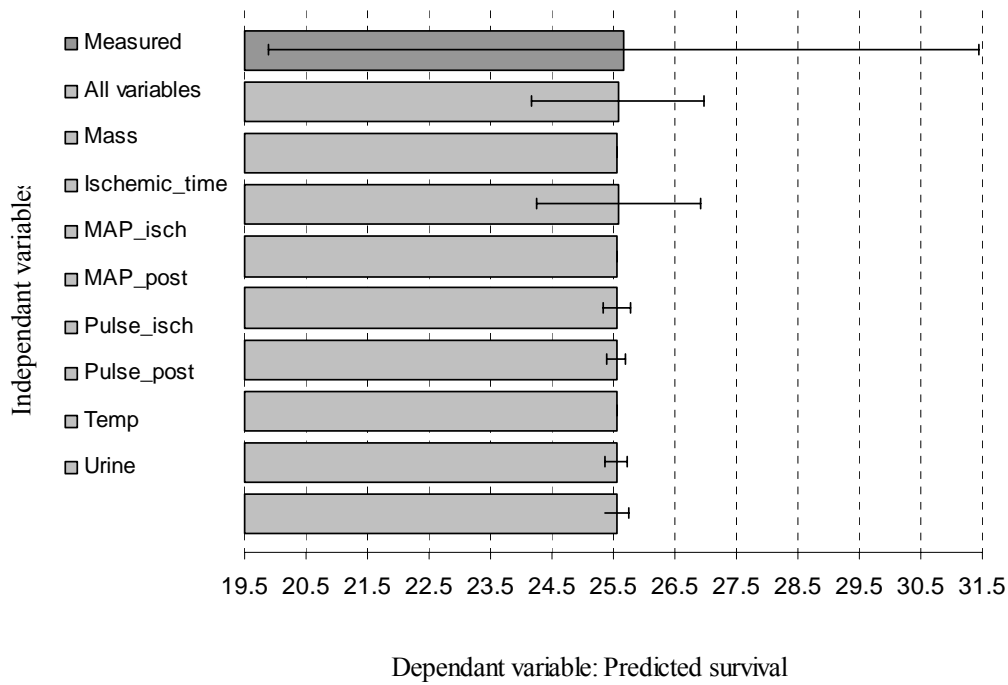


Figure D.3.5 PI Model (T<0) prediction variation using normal distributions (N=1000) of independent variables. The majority of variation in model output originated with the Ischemic_time. All input variables individually very closely approximated the measured mean.

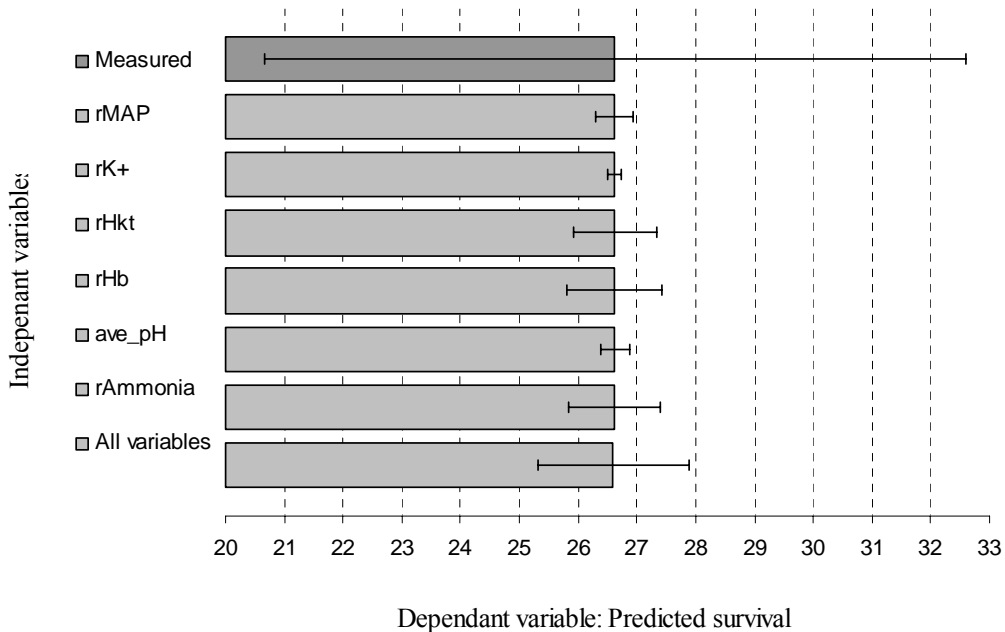


Figure D.3.6 PI Model (T>0) prediction variation using normal distributions [N=1000] of independent variables (T>0). All inputs very closely estimated the measured mean. There was a similar amount of variation in prediction from rAmmonia, rHkt and rHb.

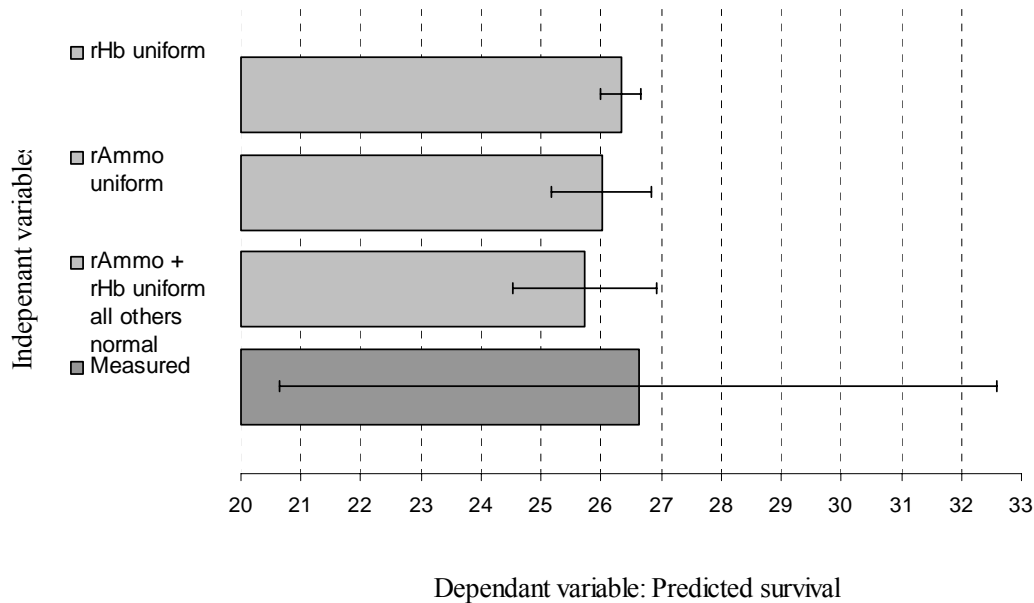


Figure D.3.7 PI Model ($T > 0$) prediction variation using uniform distributions ($N=1000$) of non-Gaussian variables. Survival was slightly underestimated when the distributions were uniform as opposed to normal.

D.4 Assumptions of normality

The measured raw data for the input variables was tested for normality using Shapiro-Wilk tests with $P(W)$ values as are available in Statistix 8 (table 5.2.7). Despite the small population sizes, it was only in the derived variables rHb and rAmmo (PI model) that normality was excluded in the $P(W)$ values, using the population from which the model's equations had been derived. To examine the effect that non-normal distributions would have on model predictions, the inputs in question were also randomized using uniform distributions. The duration of survival was marginally underestimated in the PI.

Table D.4.1 Normality of independent variables in the PI

Variable	Time period	Shapiro Wilk W-value	P(W) value	Number of cases
Survival	T<0	0.8834	0.1705	9
Body weight		0.9485	0.6738	9
Ischemic time		0.8502	0.0749	9
MAP_isch		0.9082	0.3414	8
MAP_post		0.9767	0.9454	9
MAP_post		0.9191	0.4224	8
Pulse_isch		0.9737	0.9257	8
Pulse_post		0.8442	0.0644	9
Temp_post		0.9063	0.2906	9
Urine_oper				
Survival	T>0	0.8925	0.2471	8
rMAP		0.9572	0.9353	8
ave_pH		0.9816	0.9703	8
rK+		0.8727	0.1602	8
rHkt		0.8769	0.1758	8
rHb		0.6765	0.0012	8*
rHb		0.6204	0.0001	12 [†]
rAmmonia		0.7065	0.0027	8*
rAmmonia		0.8200	0.0160	12 [†]

Notes:

1. As the W-value approaches 1, the distribution approaches normality.

If the P(W) value is < 0.05, normality may not be assumed.

2. In the T<0 part of the model all distributions indicated normality.

3. In the T>0 part of the model, only in rHb and rAmmo could normality not be assumed based on the P(W) values in both sets of data.

* Indicates the data sets (N=8) from which the model was initially defined.

† Indicates all the data sets measured (N=12).

4. The effect of non-normal distributions on model prediction variation was tested by means of employing uniform distributions for the above variables (figure 5.2.10).

5. The BI is derived from independent variables present in the T>0 part of the PI. The nature of the distributions of those variables will thus also determine prediction variation in the BI.

Table D.5.1 The number of independent variables used to calculate each biochemical in the BI

	Number of independent variables			
	4	3	2	1
Variable	BcAA/AroAA	ALP	Glutamine	Bilirubin
	Fibrinogen		Antithrombin	PT
	Creatinine		LD	Factor II, VII, X
				Factor AST ALT Urea

Notes:

1. The greater the number of weighted input variables the greater the likelihood of prediction accuracy.
2. Due to being determined by only one independent variable, the clotting factors and two of the liver enzymes, are unlikely to be predicted with great accuracy. Unfortunately, at the time of writing, there were no *on-line* sensors for these variables.

D.6 Model Verification methods and results

D.6.1 ANOVA

a. A statistical mean and standard deviation for all measured and predicted values was calculated (columns 4 and 5, table D.6.1). From this a percentage deviation of each predicted mean and standard deviation from each measured mean and standard deviation was calculated (column 6). Bearing in mind the large numerical range of measurement in the biochemical variables it was found that the predicted standard deviations about each mean differed to a greater extent than that in the measured. The greatest error was found in Factor X with a – 4.291 % difference. The percentage error for urea was 280.936%, and those for creatinine and glutamine were also unacceptably large.

b. An ANOVA comparison, using a ‘single factor without replication’ method on a 0.05 confidence level, was drawn between all predicted and measured populations. The variance in the predicted (above) and measured (below) populations was similar (column 7). In general, the variance in the predicted population was greater than in the measured, with the largest differences in urea, glutamine and creatinine once again. The mean square values (column 8) indicated that sources of variation were less between populations than within them. F-ratios were uniformly smaller than F-crit values, indicating that the differences were best explained by chance. The confidence (P) values (column 10) were mostly above 0.8, with the exception of fibrinogen, AST and LD, whose P values were below 0.55. However, all were far above 0.05, thus, the null hypothesis was rejected. Thus, it was not possible to detect a significant difference between the two populations in any of the parts of the model.



Table D.6.1 ANOVA results for the PI and BI model/s (highlighted variables were discarded)

1. Model Output	2. Pearson Correlation coefficient: predicted to measured	3. Output correction formula	4. Measured: Mean Std dev	5. Predicted: Mean Std dev	6. Percentage deviation of predicted (mean & std dev) from measured	7. Variance: Predicted over Measured.	8. Mean Square (MS): between & within grps.	9. F value & F-crit value.	10. P value ($\alpha =$ 0.05)
Prognosis T<0	0.733	y=0.1913x+20.636	24.88 5.64	25.07 7.69	0.14 4.24	59.08 31.84	0.15 45.46	0.003 4.60	0.956
Prognosis T>0	0.864	y=0.2823x+19.109	26.63 5.98	26.63 6.92	0.001 2.39	47.82 35.70	5.33x10 ⁻⁶ 41.76	1.28x10 ⁻⁷ 4.60	0.999
BcAA/AroAA	0.811	y=0.6624x+1.3662	1.98 0.75	2.03 0.90	1.27 45.88	0.86 0.57	1.94x10 ⁻⁸ 0.72	2.71x10 ⁻⁸ 4.03	0.999
BilirubinTOT	0.864	y=1.27x +3.9589	12.41 7.49	13.30 9.24	-0.91 7.28	8.34 56.07	13.74 71.13	0.19 3.98	0.662
Fibrinogen	0.962	y=1.1821x-0.8357	1.96 0.71	1.72 0.74	2.12 27.84	0.55 0.51	0.59 0.53	1.11 4.07	0.297
PT	0.945	y=0.8624x+4.4398	15.39 5.24	16.12 6.57	-0.41 4.31	43.14 27.44	8.82 35.76	0.25 3.99	0.621
AntiThrombin	0.841	y= 0.6329x +28.5	65.98 20.18	65.98 23.99	0.04 1.21	575.56 407.13	1.11x10 ⁻⁴ 491.35	2.26x10 ⁻⁷ 4.01	0.999
Factor II	0.847	y=0.7741x+8.3169	32.60 13.86	32.60 16.36	-0.03 2.46	267.50 192.09	1.75x10 ⁻⁶ 229.8	7.62x10 ⁻⁹ 3.99	0.999
Factor VII	0.837	y=0.6739x+14.753	30.35 19.40	30.35 23.18	-0.38 3.83	537.21 376.47	6.82x10 ⁻⁵ 456.84	1.49x10 ⁻⁷ 3.99	0.999
Factor X	0.786	y=0.6641x+24.718	28.96 27.11	28.96 34.51	-4.29 22.40	1.19x10 ³ 735.03	3.56x10 ⁻⁵ 962.96	3.69x10 ⁻⁸ 3.99	0.999
ALP	0.747	y=0.4547x+170.63	330.65 260.53	344.56 348.78	-0.10 0.47	1.22x10 ⁵ 6.79x10 ⁴	3.39x10 ³ 9.56x10 ⁴	0.04 3.98	0.851
AST	0.810	y= 0.763x +1306	1521.16 2025.67	1871.04 2627.43	-0.51 1.13	6.90x10 ⁶ 4.10x10 ⁶	2.04x10 ⁶ 5.61x10 ⁶	0.36 3.99	0.549
LD	0.800	y=0.7057x+949.87	1673.18 1545.16	2020.51 2230.23	-0.03 0.11	4.97x10 ⁶ 2.39x10 ⁶	2.08x10 ⁶ 3.74x10 ⁶	0.56 3.98	0.459
ALT	0.729	y=0.5878x+88.486	120.0 113.81	126.88 151.95	-0.25 1.69	2.31x10 ⁶ 1.30x10 ⁴	814.64 1.83x10 ⁴	0.05 3.98	0.833
Creatinine	0.522	y=0.4318x+82.663	129.55 53.27	129.55 101.95	0.15 1.72	1.04x10 ⁴ 2.84x10 ³	3.74x10 ⁻⁴ 6615.82	5.65x10 ⁻⁸ 3.99	0.999
Urea	0.164	y= 0.074x +2.391	2.24 0.87	2.31 5.17	-3.66 280.94	26.70 0.75	0.09 13.91	6.46x10 ⁻³ 13.91	0.936
Glutamine	0.463	y= 0.267x +178.8	207.68 96.39	207.71 207.95	-0.05 1.10	4.32x10 ⁴ 9.28x10 ³	9.14x10 ⁻³ 2.63x10 ⁴	3.48x10 ⁻⁷ 4.01	0.999

D.6.2 Relative error

a. The error of each predicted to corresponding measured value was calculated as a fraction of each measured value. i.e. the deviation at a particular point or *point error*. This was divided by the standard deviation of the measured population and converted to a percentile scale to give the *relative error* for each part of the model. If the *point error* exceeded 100% of the standard deviation of the measured population, then there was a significant difference between the two populations at that point. In general, the closer the mean relative error value to zero, the closer the model has estimated the mean of the measured population, while the standard deviation of the relative error (*SD_{re}*) indicates the predicted population's range of error.

A potential weakness in this method was that when a variable demonstrated a very large numerical range over the course of an experiment, the relative error would tend to be larger in the small range and smaller in the large range of the raw data. i.e. the relative error converged to zero as the measurement range increased. This effect was only noticeable in the liver enzymes in which there were extremely large measurement ranges (from 0-7000 IU/l). These enzymes have no prognostic value in ALF and for this reason the effect could have been ignored. However, for the sake of thoroughness,

b. A quantitative index for comparison was calculated by multiplying the measurement range with the standard deviation of the relative error (*SD_{re}*) (table D.6.2.1). The larger the returned value, the larger the prediction *error region*. This represents a method of indicating the *average relative accuracy* of the various parts of the model. What must be borne in mind, especially in the biochemical variables, is that although the deviation in the relative error may have been small, the measured value range was often very large. In practice the point errors may still have been large.

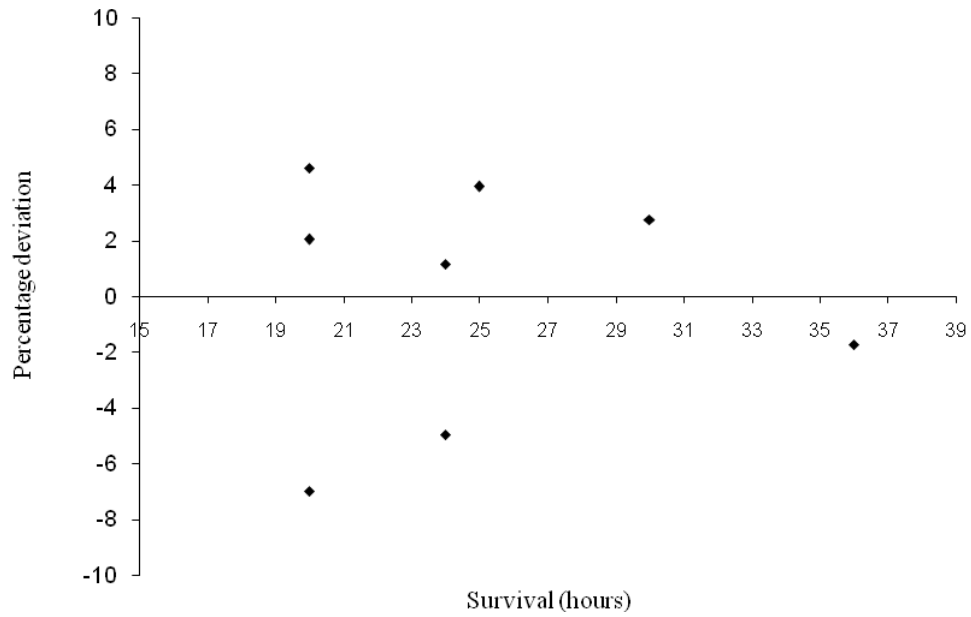


Figure D.6.2.1 Relative prediction error for the PI ($T < 0$)

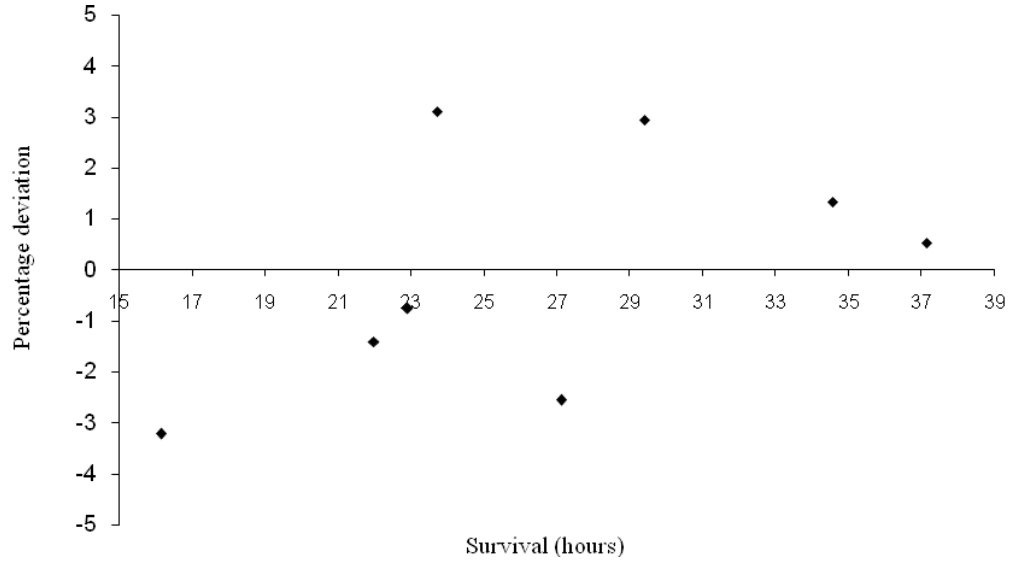


Figure D.6.2.2 Relative error for PI ($T > 0$)

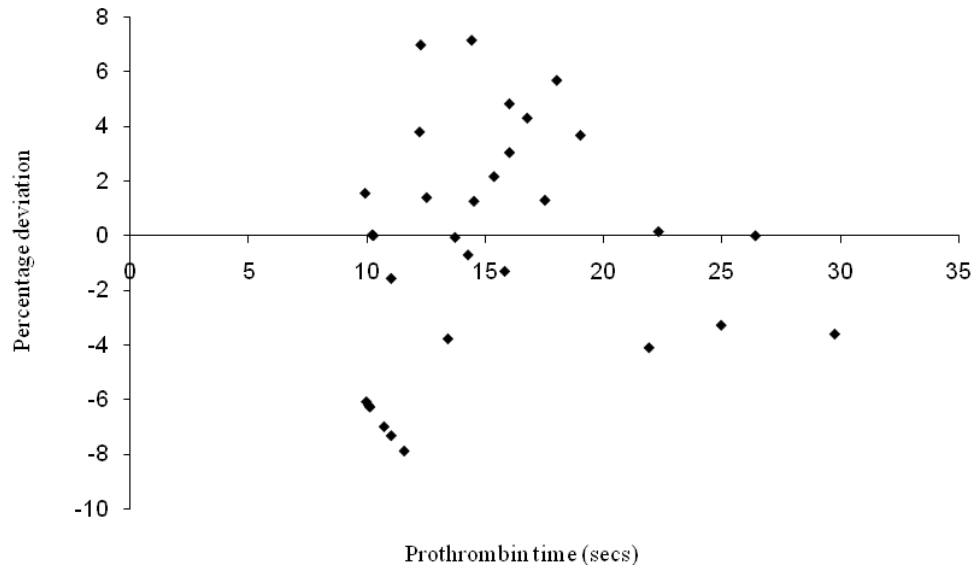


Figure D.6.2.3 Relative error for the BI (Prothrombin time)

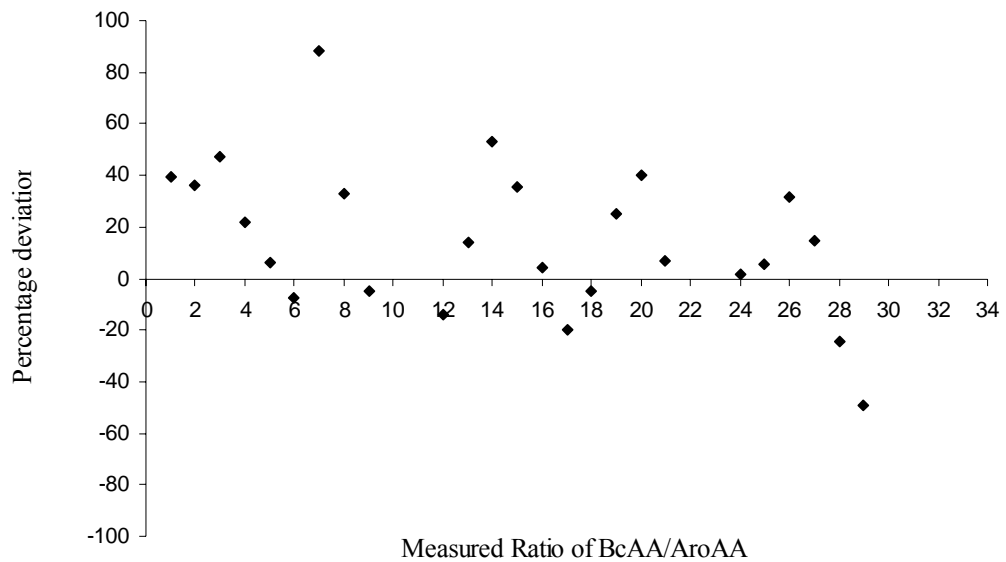


Figure D.6.2.4 Relative error for the BI [BcAA/AroAA]



Table D.6.2.1 Comparative accuracy of the PI and BI models (using ‘training’ data)

Model Index	Measured values			Accuracy Index		
	Max	Min	Range	Mean	SD _{re}	Range*SD _{re}
Prognosis T<0	36	20	16	0.14	4.24	67
Prognosis T>0	36	20	16	0.001	2.39	38
BcAA/AroAA	3.75	1.19	2.55	1.67	29.00	48.43
BilirubinTOT	30.0	1.0	29.0	-0.91	7.28	211.2
Fibrinogen	2.97	0.50	2.47	2.12	27.84	68.76
PT	29.75	9.90	19.85	-0.41	4.31	85.49
AntiThrombin	112.89	14.00	98.89	0.04	1.21	119.44
Factor II	59.65	7.61	52.04	-0.03	2.46	127.87
Factor VII	74.95	6.19	68.76	-0.08	3.28	225.54
Factor X	104.96	1.00	103.96	0.98	3.94	409.93
ALP	1206.0	57.0	1149.0	-0.01	0.32	366.9
AST	6607.0	23.0	6584.0	0.01	0.07	441.1
LD	6161.0	155.0	6006.0	-0.001	0.05	301.2
ALT	377.0	23.0	354.0	0.15	1.15	405.2
Creatinine	284.8	11.5	273.3	0.15	1.72	468.8
Urea	4.6	1.6	3.2	67.71	173.81	556.2
Glutamine	445.0	76.8	368.2	0.63	0.94	344.2

Notes:

1. *SD_{re} = Standard deviation of the relative error
2. The closer the mean prediction error to 0, the closer the mean measured value has been estimated.
3. The smaller the Range*SD_{re} the smaller the *error region* and the more accurate the predictions.

Acknowledgements

Prof. Schalk W van der Merwe. With your help in these last 8 years I have grown both as a person and in professional capacity as a scientist. Thank you for the opportunity in the first place to participate in this project, without it none of what was subsequently built would have been possible. Thank you for your belief in my abilities, for the positive words to colleagues and for the many times you intervened on my behalf, especially when the resulting outcomes would have been impossible without your help (there are simply too many to list). Thank you for your objective and invariably strategically useful advice, no matter what the subject.

Dr Pierre Cilliers and Prof. JJ Kruger. Thank you for identifying the necessity, your belief in and excellent tutorship for my particular tangent through the sciences. I will certainly try to keep the flame burning. **Prof. P de Vaal.** I realize I was sort of ‘forced’ on you. Thank you for taking over where the others left off. I hope I am able to do you duty in any future endeavours.

Kobus van Wyk, Luke Ronné, Susan Malfeld, Elke Kreft and Elongo Fritz. Thank you for your individual and collective efforts in trying to realize these projects of ours. It is obvious that any success I may have achieved is at least partially dependent on your inputs. In terms of my career, the years we have worked together have been the most enjoyable I have experienced.

Dr Sean Moolman, Kersch Naidoo. Thank you for your always interesting and insightful inputs, especially regarding the commercial side of things. I am grateful for the continued enthusiasm you have displayed for all our projects, our relationship remains productive and pleasurable.

Prof Johan Becker, Dr Scholz Wiggett, Dr Roland Auer and the staff of the UPBRC. Thank you for your help and interest in our projects. Your participation has been critical to our success.

My parents, Ben and Betty Nieuwoudt. Your belief in me kept me going, especially when circumstances were difficult. This thesis is dedicated to you.